

This is an Open Access document downloaded from ORCA, Cardiff University's institutional repository:<https://orca.cardiff.ac.uk/id/eprint/167890/>

This is the author's version of a work that was submitted to / accepted for publication.

Citation for final published version:

Wang, Jun, Xu, Jian, Wang, Jingjing, Ke, Deping, Yao, Liangzhong, Zhou, Yue and Liao, Siyang 2024. Two-stage distributionally robust offering and pricing strategy for a price-maker virtual power plant. *Applied Energy* 363 , 123005. 10.1016/j.apenergy.2024.123005

Publishers page: <http://dx.doi.org/10.1016/j.apenergy.2024.123005>

Please note:

Changes made as a result of publishing processes such as copy-editing, formatting and page numbers may not be reflected in this version. For the definitive version of this publication, please refer to the published source. You are advised to consult the publisher's version if you wish to cite this paper.

This version is being made available in accordance with publisher policies. See <http://orca.cf.ac.uk/policies.html> for usage policies. Copyright and moral rights for publications made available in ORCA are retained by the copyright holders.



Two-stage distributionally robust offering and pricing strategy for a price-maker virtual power plant

Jun Wang, Jian Xu, Jingjing Wang, Deping Ke, Liangzhong Yao, Yue Zhou, and Siyang Liao

Abstract—This paper presents a two-stage distributionally robust approach for offering and pricing strategy of a virtual power plant (VPP) acting as a price-maker in the day-ahead market. The model incorporates uncertainties related to distributed photovoltaic (PV) output, real-time market price and charging stations demand. In the first stage, the VPP determines its day-ahead market bids/offers as a price maker and releases the retail price to the charging stations based on the worst case of probability distribution realizations. In the second stage, the VPP optimizes energy storage operations and the power transactions in the real-time market to maximize its revenue according to the optimal first stage decisions. To efficiently solve the two-stage model, a customized column-and-constraint generation algorithm (C&CG) is designed that decomposes non-convex subproblems into several small-scale linear programming problems that are independent of each other. The effectiveness of the proposed strategy is validated through case studies conducted with the IEEE 33-bus system.

Index Terms—Virtual power plant, price maker, dynamic pricing, distributionally robust, electric vehicle

NOMENCLATURE

A. Sets and Indices

t, s	Index for time intervals, scenarios, respectively
r / Ω^{RN}	Index / set for renewable energy sources
i, j	Indices for nodes of the virtual power plant
c / Ω^{CS}	Index / set for EV charging stations
n / Ω_c^{EV}	Index / set for EVs at charging station c
$e / \Omega_c^{\text{ESS}}$	Index for energy storage
$l / \Omega_i^{\text{LN},e/s}$	Index / set of lines within virtual power plant
k	Index for iterations

B. Parameters

θ_1, θ_e	Tolerance value of probability distribution deviation
$p_{t,c}^{\text{ret,min/max}}$	Retail price limits issued to charging station c
$p_t^{\text{buy/sell,max}}$	Maximum bidding quantity value for VPP
p_c^{av}	Maximum average retail price value
$V^{\text{max/min}}$	Maximum / minimum voltage amplitudes
$P_{s,l,t}^{\text{LN,max/min}}$	Maximum / minimum power transmission limits
$P_e^{\text{ESS,max}}$	Maximum charging/discharging power of ESS
$\eta_e^{\text{ESS, ch/dis}}$	Charging/discharging efficiency of ESS e
E_0^{ESS}	Initial energy stored in ESS
$P^{\text{RT,max}}$	Maximum trading value in real-time market
$P_{c,t}^{\text{CS,max}}$	Maximum available charging/discharging power of charging station c
$E_{c,t}^{\text{CS,max/min}}$	Equivalent energy boundary of charging station c

This work was supported by the National Key Research and Development Program of China under Grant 2022YFB2403500. (*Corresponding author: Jian Xu*).

Jun Wang, Jian Xu, Jingjing Wang, Deping Ke, Siyang Liao and Liangzhong Yao are with the School of Electrical Engineering and Automation, Wuhan University, Wuhan, 430072 China.

(email: wangjun@whu.edu.cn; xujian@whu.edu.cn; wangjingjing@whu.edu.cn; kedeping@whu.edu.cn; liaosiyang@whu.edu.cn; yaoliangzhong@whu.edu.cn).

Yue Zhou is with the School of Engineering, Cardiff University, Cardiff, UK (email: zhouy68@cardiff.ac.uk).

$\Delta E_{c,t}^{CS}$	Equivalent energy change of charging station c
T_n^a / T_n^d	Arrival / departure times of EV n
E_n^a / E_n^d	Initial and expected energy set by EV n
$P_{i,t}^{LD} / Q_{i,t}^{LD}$	Active / reactive power of uncontrollable loads
$M_{i,r}^{RN} / M_{i,c}^{CS}$	Incidence matrices for PVs / charging stations
p_t^{penalty}	Penalty cost coefficient

C. Variables

$p_{1,c}^{\text{ret}}$	Retail price issued to charging station c
π_s	Probability distribution of PV forecast error, uncertain variable
$P_t^{\text{bid/offer}}$	Quantity bids for VPP as a consumer or producer
$P_{s,t}^{\text{RT,buy}}$	Purchased power of VPP in the real-time market
$P_{s,t}^{\text{RT,sell}}$	Sold power of VPP in the real-time market
$P_{s,e,t}^{\text{ESS,ch}}$	Charging power of ESS e at time t
$P_{s,e,t}^{\text{ESS,dis}}$	Discharging power of ESS e at time t
$E_{s,e,t}^{\text{ESS}}$	The stored energy of ESS e at time t
$P_{c,t}^{\text{CS,ch}}$	Charging power of charging station c at time t
$P_{c,t}^{\text{CS,dis}}$	Discharging power of charging station c at time t
$P_{s,r,t}^{\text{RN}}$	Active generation power of PV r
$Q_{s,t}^{\text{NE}}$	Net reactive exchange power
I_t^{EM}	Binary variable indicating VPP bids as a producer or consumer
$I_{s,t}^{\text{RT}}$	Binary variable indicating VPP purchase or sell energy in the real-time market
$P_{s,l,t}^{\text{LN}}, Q_{s,l,t}^{\text{LN}}$	The active and reactive power of branch l within the VPP
$P_{s,l,t}^{\text{LS}}, Q_{s,l,t}^{\text{LS}}$	The active and reactive power loss of branch l within the VPP
$V_{s,i,t}$	The voltage of node i within the VPP

I. INTRODUCTION

With a significant integration of distributed energy resources (DERs) into the power grid, including electric vehicles (EVs), distributed renewable energy sources and energy storage, etc., the effective management and rational utilization of these DERs have gained increased importance. The virtual power plants (VPPs) which act as a party that realizes aggregation, optimization and control of DERs are emerging [1]. Especially under the electricity market environment, a single DER as a market participant cannot meet the minimum capacity requirement (typically 1 megawatt in China) stipulated by the market operator. Besides, the market clearing would be a huge burden if so many DERs usually located in low-voltage level power grid all directly participate in the market as independent market entities. Therefore, VPP that participates in the wholesale market by aggregating and managing DERs has been generally considered as a promising technology.

There are usually two main types of VPP in existing researches, i.e., technical virtual power plant (TVPP) [2] and commercial virtual power plant (CVPP) [3]. The TVPPs can combine various DERs located in the same geographic area to produce an aggregated overall output that closely resembles that of conventional power plants [4][5]. The CVPPs mainly focus on aggregating multiple DERs across geographic scales to reduce total output uncertainty [6], they usually have their own regional networks and participate in the power market through a grid connection point [7]. In this paper, the VPP's structure primarily aligns with the latter one, focusing on trading energy in both the day-ahead and real-time market on behalf of end-users and settles based on the market clearing price. At the same time, it makes settlement with the end-users according to the retail price released by itself, thus arbitrages based on the price difference. Based on whether the impact of VPPs' bidding strategies on market clearing prices is considered, they are typically classified into two categories: price taker [8][13] and price maker [9]-[12]. Rahimiyan *et al.* introduced a two-

stage robust model for optimizing the bidding strategy of a price-taker VPP in both the day-ahead and real-time market [8]. Liu *et al.* presents a hybrid stochastic/robust optimization approach to gain the bidding strategy for a price-taker microgrid in the day-ahead market [13]. Price-maker strategies provides a higher number of arbitrage opportunities for maximizing revenue compared with the price-taker models.

Based on the information available to the market participants, the current researches in the field of price-maker strategies can be classified into three main categories: mathematical program with equilibrium constraints (MPEC) [14][15], game theory based methods [16] and residual energy curve (REC) based methods [9]-[12],[17]. Y. Ye *et al* presents a bi-level optimization approach to examine the positive impact of energy storage on constraining market power of generation companies and they solved the model by converting it to a MPEC [15]. In [16], the complex bidding issue of multiple VPPs is addressed through the formulation of a multi-leader-follower game model. The model serves as a framework to determine the optimal contract prices for VPPs and it involves competition among VPPs at the upper level. Hu *et al.* proposed a bidding model for a price-maker microgrid which enables the determination of hourly bidding/offering curves in the day-ahead market. The model considers the uncertainty of REC curves [17]. Nonetheless, the arbitrage opportunities in the real-time market were ignored in [17]. In this paper, the VPP is assumed to participate in the day-ahead market as a price-maker while the real-time market as a price taker.

It has been shown that above existing discussions on bidding/offering strategies for VPPs mostly assume that they have direct scheduling rights over the flexible load resources. However, VPPs without the rights can still offer electricity to the end-users at an alternative retail price which they have the flexibility to modify [32]. Yao *et al* introduced a dynamic pricing strategy for microgrids using a Stackelberg game model. The model could offer unique load prices for individual users by considering their satisfaction feedback [18]. Wei *et al* firstly developed a two-stage optimization framework to address the challenges of retail price determination and energy dispatch strategies for an electricity retailer under the real-time market price uncertainty [32]. Xu *et al* explored a pricing strategy for load aggregators based on data-driven methods, which can achieve the coordination of energy consumption between aggregators and end-users [21]. However, the above studies only focus on the pricing strategy for a market entity while ignore its strategic behaviors in the day-ahead market. In recent years, some researches model the coordinated bidding problem in the wholesale market and the pricing problem in the retail market. In [19], a personalized retail pricing strategy for various consumers is designed based on a bi-level optimization model. The upper-level models the retailer's price decision-making problem, the lower-level models the users' demand response and the day-ahead wholesale market clearing problem. Based on [19], the real-time market clearing is further modeled as another lower-level problem in [20]. Both of them primarily focus on the wind power uncertainty in the wholesale market, and do not consider the uncertainties of the internal distributed renewable energy within the market entity.

To sum up, this paper tries to comprehensively address the bids/offers and retail price decision-making problem considering the influence of VPP's bids/offers on the market clearing, which is different from [32]. In our work, the VPP, functioning as a price-maker, decides its day-ahead bids/offers and releases the retail price to the charging stations in the first stage. In the second stage, the VPP optimizes the energy storage operations and power transactions to maximize the revenue in the real-time market. The main contributions of this paper are as follows:

(1) A two-stage distributionally robust bi-level optimization model for offering and pricing strategy of VPP is proposed. The model incorporates uncertainties related to distributed PV output, real-time market price and the charging stations demand. It can capture the impact of VPP's offering on market clearing price and ensure the VPP make the optimal decisions under the worst case of probability distribution realizations.

(2) A customized C&CG algorithm is developed to efficiently solve the two-stage model. There is no need for primal-dual transformation of subproblems. By further decomposing the non-convex subproblems into several small-scale linear programming problems that are independent of each other, the parallel computing can be used to speed up the solution efficiency.

The rest of this paper is structured as follows. Section II presents the overall framework. Section III details the uncertainties modeling methods and the two-stage bi-level optimization model. Section IV gives the model reformulation and the solution method. Section V presents the case study. Finally, Section VI draws the conclusion.

II. FRAMEWORK

The structure of the VPP and its interactions with the market are shown in Fig.1. The VPP acts as an aggregator of electric vehicle charging stations (EVCS), energy storage systems (ESS) and photovoltaic stations (PV). It operates as

a price-maker, submitting bids/offers to the superior power market operator. Meanwhile, it owns a regional network topology and serves as an intermediary entity connecting the power market with consumers through a point of common coupling (PCC) [28]. On the one hand, the VPP formulates the day-ahead hourly bidding strategies presented to the market and designs the retail price to the electric vehicle consumers. Therefore, the VPP is required to release the retail pricing information to consumers a day in advance. On the other hand, due to its possession of ESS, the VPP can engage in real-time market to buy/sell electricity to compensate for imbalances between the day-ahead energy contracts and the real-time consumption. Furthermore, the VPP agent is tasked with the responsibility of maintaining internal power balance and effectively managing congestion to ensure the system security. Given the uncertainties related to PV output and the real-time market electricity price, the VPP should design reasonable retail pricing strategies, aiming to not only maximize its profit but also minimize potential financial risks to the greatest extent possible. To achieve these goals, we propose a two-stage distributionally robust offering and pricing strategy to achieve the revenue maximization of the VPP, which can function as a prosumer (capable of transitioning between the roles of a producer and a consumer) and a price-maker. A data-driven uncertainty set is employed to depict the potential realizations of the probability distribution of PV output, which does not necessitate the precise knowledge of the PV output probability distributions. The decision-making processes of the VPP contain four parts, as shown in Fig.2.

1) *Day-ahead offering and the retail price determination*: The VPP operates as a price maker in the power market, it should decide the optimal quantity bid in the market and the retail prices offered to its served EVCSs. These decisions are made under the uncertainties of PV output, charging stations' demand and the electricity price.

2) *Power imbalance regulation in real-time market*: Upon the market's declaration of the clearing result, the VPP proceeds to optimize the operation of the ESS and the real-time electricity transactions based on the users' demand response to the retail price, aiming to regulate the imbalances between the day-ahead contract and actual consumption.

3) *Day-ahead market clearing process*: The market operator performs market clearing based on the bids/offers from all participants, aiming to maximize the social welfare. However, due to the privacy protection and fairness promoting, it is remarkably difficult for a VPP to obtain competitor's bidding plans. In this paper, we employ the residual energy curve method to simplify the market clearing process.

4) *Demand response*: Once the VPP releases the retail prices, its served EVCSs do demand response to maximize their own profits. Their energy consumption schemes can be considered as highly correlated with retail prices.

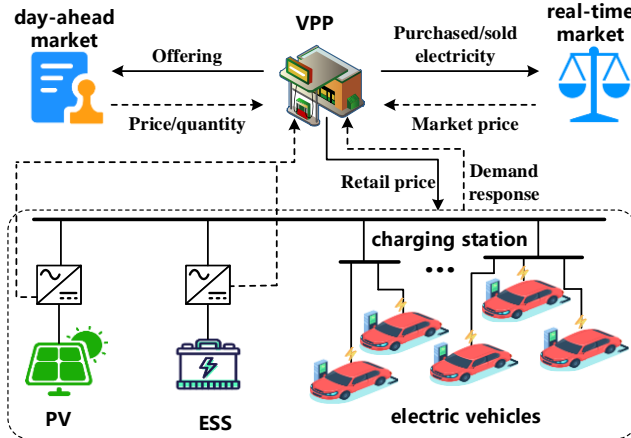


Fig. 1. The structure of VPP participating in the day-ahead and real-time market.

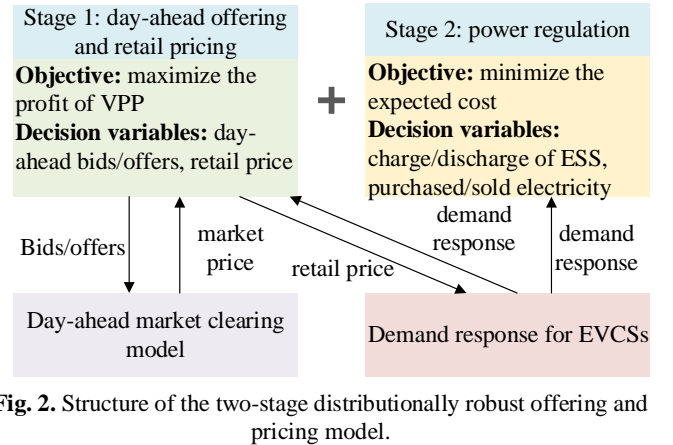


Fig. 2. Structure of the two-stage distributionally robust offering and pricing model.

III. MATHEMATICAL FORMULATION

The VPP in this paper is assumed to be a price-maker in the day-ahead market and a price-taker in the real-time market with the goal of maximizing its net revenue. The electricity price of real-time market and distributed PV power uncertainties are described through scenario-based method and ambiguity sets, respectively. Then a two-stage bi-level distributionally robust offering and pricing strategy for a VPP is proposed.

A. Modeling Uncertainties

The price-maker day-ahead offering and pricing strategy formulation for a VPP are affected by multiple uncertainties, such as the market clearing price, the distributed PV power and the load demand. To deal with the random variables,

there are usually two types of methods, i.e., probability distribution based method [22] and scenario-based method [23]. The former one requires to know precise knowledge of random variables' probability distributions, and the unanalytical characteristics of the inverse functions of most probability distributions would make optimization problems difficult to solve. Besides, for the scenario-based methods, the probability distribution of generating scenarios would also be uncertain due to the sampling errors in scenario generation, which is generally ignored in existing researches. In this paper, the distributed PV power and real-time market price uncertainty is addressed by a scenario-based method firstly, then the probability distribution uncertainty of scenarios is characterized by a distributionally robust uncertainty set[24][25]. As for the uncertain load demand within the VPP, the reactions from consumers' responses to the price signal is considered, which are discussed in detail in Section III-C. More specifically, the Cornish-Fisher expansion technique is used to capture the approximate functional relationship between the quantile of the marginal probability distribution of the forecast error at time t and the historical forecast error samples firstly, and then the Latin Hypercube Sampling (LHS) method is used to perform random sampling at equal probability intervals. After that, we reorder the generated samples based on Cholesky decomposition to ensure that the reordered scenarios can effectively reflect the temporal correlations [26], as shown in Fig.3.

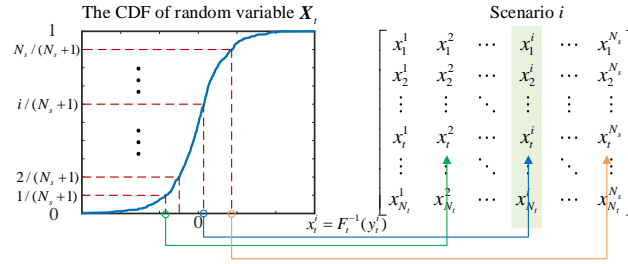


Fig. 3. The diagram of Latin Hypercube Sampling process.

After scenario reduction, we can obtain N_s typical scenarios $\Delta \mathbf{P}^0 \in \mathbb{R}^{N_t \times N_s}$ and the corresponding discrete scenario probability distribution $\boldsymbol{\pi}^0 = (\pi_1^0, \pi_2^0, \dots, \pi_{N_s}^0)$, which represent the corresponding obtained empirical distribution. Given the potential variance between the actual distribution and empirical distribution, we employ statistical inference to delineate uncertainty set that corresponds to a specific parameter $\boldsymbol{\theta}$. Specifically, we use the L_1 and L_∞ norms to measure the difference between the actual distribution and empirical distribution, as shown in (1) and (2). By using the two norms, the actual distribution could converge to the true distribution as the number of data goes to infinity.

$$\boldsymbol{\psi}_1 = \left\{ \boldsymbol{\pi} \in \mathbb{R}_+^{N_s} \mid \|\boldsymbol{\pi} - \boldsymbol{\pi}^0\|_1 \leq \boldsymbol{\theta}_1 \right\} = \left\{ \boldsymbol{\pi} \in \mathbb{R}_+^{N_s} \mid \sum_{s=1}^{N_s} |\pi_s - \pi_s^0| \leq \boldsymbol{\theta}_1 \right\} \quad (1)$$

$$\boldsymbol{\psi}_\infty = \left\{ \boldsymbol{\pi} \in \mathbb{R}_+^{N_s} \mid \|\boldsymbol{\pi} - \boldsymbol{\pi}^0\|_\infty \leq \boldsymbol{\theta}_\infty \right\} = \left\{ \boldsymbol{\pi} \in \mathbb{R}_+^{N_s} \mid \max_{1 \leq s \leq N_s} |\pi_s - \pi_s^0| \leq \boldsymbol{\theta}_\infty \right\} \quad (2)$$

where $\boldsymbol{\psi}_1$ and $\boldsymbol{\psi}_\infty$ are two types of uncertainty sets corresponding to L_1 and L_∞ norms. $\boldsymbol{\theta}_1$ and $\boldsymbol{\theta}_\infty$ are the tolerance value that probability distribution deviate from the empirical distribution [27], which can be computed according to (3).

$$\boldsymbol{\theta}_1 = \frac{N_s}{2M} \log \frac{2N_s}{1 - \alpha_1}, \quad \boldsymbol{\theta}_\infty = \frac{1}{2M} \log \frac{2N_s}{1 - \alpha_\infty} \quad (3)$$

where M is the size of historical scenarios before reduction, which is related to the bounds of the uncertainty set. α_1 and α_∞ are the confidence level corresponding to L_1 and L_∞ norms.

Therefore, the uncertainty of the probability distribution $\boldsymbol{\pi}$ is described by the following uncertainty set $\boldsymbol{\psi}$, as shown in (4).

$$\boldsymbol{\psi} = \left\{ \boldsymbol{\pi} \in \mathbb{R}_+^{N_s} \mid \begin{array}{l} \sum_{s=1}^{N_s} |\pi_s - \pi_s^0| \leq \boldsymbol{\theta}_1 \\ \max_{1 \leq s \leq N_s} |\pi_s - \pi_s^0| \leq \boldsymbol{\theta}_\infty \\ \sum_{s=1}^{N_s} \pi_s = 1 \end{array} \right\} \quad (4)$$

B. Upper Level Offering and Pricing Model of the VPP

1) *Stage 1: day-ahead offering and retail price setting.* In day-ahead stage, the market clearing price is affected by the VPP's quantity offers. Consequently, the VPP must decide its optimal day-ahead quantity offers and release the retail price to the end-users in order to maximize its own revenue. The objective function contains two parts, as shown in (5), the first and second terms represent the day-ahead market revenue, and the third term represents the revenue generated through the sale of electricity to charging stations within the VPP.

$$\max_x \Delta t \sum_{t=1}^{N_T} (p_t^{\text{clear,sell}} P_t^{\text{clear,sell}} - p_t^{\text{clear,buy}} P_t^{\text{clear,buy}} + \sum_{c=1}^{N_{CS}} p_{t,c}^{\text{ret}} (P_{c,t}^{\text{CS,ch}} - P_{c,t}^{\text{CS,dis}})) \quad (5)$$

$$\text{s.t.} \quad p_{t,c}^{\text{ret,min}} \leq p_{t,c}^{\text{ret}} \leq p_{t,c}^{\text{ret,max}}, \forall t, c \quad (6)$$

$$\sum_{t=1}^{N_T} p_{t,c}^{\text{ret}} / N_T \leq p_c^{\text{av}}, \forall c \quad (7)$$

$$0 \leq P_t^{\text{offer}} \leq I_t^{\text{EM}} P_t^{\text{sell,max}}, \forall t \quad (8)$$

$$0 \leq P_t^{\text{bid}} \leq (1 - I_t^{\text{EM}}) P_t^{\text{buy,max}}, \forall t \quad (9)$$

$$\{P_{c,t}^{\text{CS,ch}}, P_{c,t}^{\text{CS,dis}}\} = F_n^{\text{EVCS}}(p_{t,c}^{\text{ret}}), \forall t, c \quad (10)$$

where $x = \{P_t^{\text{bid}}, P_t^{\text{offer}}, p_{t,c}^{\text{ret}}, I_t^{\text{EM}}\}$ are the decision variables set at this stage. $p_t^{\text{clear,sell/buy}}$ and $P_t^{\text{clear,sell/buy}}$ represent the day-ahead market cleared price and quantity, which are both influenced by the quantity bid $P_t^{\text{bid/offer}}$ of the VPP, the details are given in the following section. $P_{c,t}^{\text{CS,ch}}$ and $P_{c,t}^{\text{CS,dis}}$ are the equivalent charging/discharging power of EVCS c , and they are the function of the retail price offered by the VPP, as in (10). The retail price offered to the EVCSs should be maintained within a certain range, as in (6). The average value of the retail price should not exceed the allowable value, as in (7). The VPP needs to decide whether to participate in the market as a produce or a consumer according to (8) and (9), I_t^{EM} is a binary variable, $I_t^{\text{EM}}=1$ means it bids as a producer in supply side and $I_t^{\text{EM}}=0$ means it bids as a consumer in demand side.

2) *Stage 2: energy dispatching problem.* In this stage, the VPP optimizes the energy storage system's charging/discharging operations and the electricity transactions in the real-time market based on the energy consumption plans of the charging stations. To mitigate the potential risks arising from the uncertainty of probability distribution, the VPP seeks to maximize the revenue in the worst case of PV output probability distribution realizations. The energy dispatch problem is formulated as a min-max form related to the worst case of probability distribution realization, as shown in (11). The first term is the real-time power sales revenue, the second term is the power purchase cost from the real-time market and the last two terms are the penalty cost due to the deviations from the day-ahead contract.

$$\min_{\{\mathbf{x}\} \in \Psi} \sum_{s=1}^{N_s} \pi_s \max_{y_s} \sum_{t=1}^{N_T} (p_{s,t}^{\text{RT}} (P_{s,t}^{\text{RT,sell}} - P_{s,t}^{\text{RT,buy}}) + p_t^{\text{penalty}} (P_{s,t}^{\text{RT,sell}} + P_{s,t}^{\text{RT,buy}})) \quad (11)$$

$$\text{s.t.} \quad M_i^{\text{NE}} (P_t^{\text{clear,buy}} - P_t^{\text{clear,sell}}) + \sum_{e \in \Omega^{\text{ESS}}} M_{i,e}^{\text{ESS}} (P_{s,e,t}^{\text{ESS,dis}} - P_{s,e,t}^{\text{ESS,ch}}) + \sum_{r \in \Omega^{\text{RN}}} M_{i,r}^{\text{RN}} P_{s,r,t}^{\text{RN}} + \sum_{c \in \Omega^{\text{CS}}} M_{i,c}^{\text{CS}} (P_{c,t}^{\text{CS,dis}} - P_{c,t}^{\text{CS,ch}}) - P_{i,t}^{\text{LD}} + \quad (12)$$

$$M_i^{\text{NE}} (P_{s,t}^{\text{RT,buy}} - P_{s,t}^{\text{RT,sell}}) = \sum_{l \in \Omega_s^{\text{LN,s}}} P_{s,l,t}^{\text{LN}} - \sum_{l \in \Omega_s^{\text{LN,e}}} (P_{s,l,t}^{\text{LN}} - P_{s,l,t}^{\text{LS}}), \forall s, i, t$$

$$M_i^{\text{NE}} Q_{s,t}^{\text{NE}} - Q_{i,t}^{\text{LD}} = \sum_{l \in \Omega_s^{\text{LN,s}}} Q_{s,l,t}^{\text{LN}} - \sum_{l \in \Omega_s^{\text{LN,e}}} (Q_{s,l,t}^{\text{LN}} - Q_{s,l,t}^{\text{LS}}), \forall s, i, t \quad (13)$$

$$V_{s,i,t}^2 - V_{s,j,t}^2 = 2(R_l P_{s,l,t}^{\text{LN}} + X_l Q_{s,l,t}^{\text{LN}}) - (R_l^2 + X_l^2)((P_{s,l,t}^{\text{LN}})^2 + (Q_{s,l,t}^{\text{LN}})^2) / V_{s,i,t}^2, \forall s, l, t \quad (14)$$

$$V^{\text{min}} \leq V_{s,i,t} \leq V^{\text{max}}, \forall s, i, t \quad (15)$$

$$P_{s,l,t}^{\text{LN,min}} \leq P_{s,l,t}^{\text{LN}} \leq P_{s,l,t}^{\text{LN,max}}, \forall s, l, t \quad (16)$$

$$Q_{s,l,t}^{\text{LN,min}} \leq Q_{s,l,t}^{\text{LN}} \leq Q_{s,l,t}^{\text{LN,max}}, \forall s, l, t \quad (17)$$

$$0 \leq P_{s,e,t}^{\text{ESS,ch}} \leq P_e^{\text{ESS,max}} I_{s,t}^{\text{ESS}}, \forall s, e, t \quad (18)$$

$$0 \leq P_{s,e,t}^{\text{ESS,dis}} \leq P_e^{\text{ESS,max}} (1 - I_{s,t}^{\text{ESS}}), \forall s, e, t \quad (19)$$

$$E_{s,e,t}^{\text{ESS}} = E_{s,e,t-1}^{\text{ESS}} + \eta_e^{\text{ESS,ch}} P_{s,e,t}^{\text{ESS,ch}} \Delta t - P_{s,e,t}^{\text{ESS,dis}} \Delta t / \eta_e^{\text{ESS,dis}}, \forall s, e, t \quad (20)$$

$$E_{\text{min}}^{\text{ESS}} \leq E_{s,e,t}^{\text{ESS}} \leq E_{\text{max}}^{\text{ESS}}, \forall s, e, t \quad (21)$$

$$E_{s,e,1}^{\text{ESS}} = E_{s,e,N_T}^{\text{ESS}} = E_0^{\text{ESS}}, \forall s, e \quad (22)$$

$$0 \leq P_{s,t}^{\text{RT,sell}} \leq P_{s,t}^{\text{RT,max}} I_{s,t}^{\text{RT}}, \forall s, t \quad (23)$$

$$0 \leq P_{s,t}^{\text{RT,buy}} \leq P_{s,t}^{\text{RT,max}} (1 - I_{s,t}^{\text{RT}}), \forall s, t \quad (24)$$

$$0 \leq P_{s,r,t}^{\text{RN}} \leq P_{s,r,t}^{\text{RN,max}}, \forall s, r, t \quad (25)$$

where $y_s = \{P_{s,t}^{\text{RT,buy}}, P_{s,t}^{\text{RT,sell}}, P_{s,e,t}^{\text{ESS,ch}}, P_{s,e,t}^{\text{ESS,dis}}, E_{s,e,t}^{\text{ESS}}, V_{s,i,t}, P_{s,i,t}^{\text{LN}}, Q_{s,i,t}^{\text{LN}}, P_{s,i,t}^{\text{LS}}, Q_{s,i,t}^{\text{LS}}, I_{s,t}^{\text{ESS}}, I_{s,t}^{\text{RT}}\}$ are the decision variables set at this stage. $P_{s,t}^{\text{RT,buy}}$ and $P_{s,t}^{\text{RT,sell}}$ are the purchased/sold power at the real-time market for scenario s . $P_{s,e,t}^{\text{ESS,ch}}$ and $P_{s,e,t}^{\text{ESS,dis}}$ are the charging/discharging power of energy storage e , respectively. $p_{s,t}^{\text{RT}}$ is the real-time market price. $M_{i,c}^{\text{NE}}, M_{i,e}^{\text{ESS}}, M_{i,r}^{\text{RN}}$ and $M_{i,c}^{\text{CS}}$ are the node-PCC, node-ESS, node-PV and node-EVCS incidence matrices, respectively. $I_{s,t}^{\text{ESS}}$ is a binary variable, energy storage e is at charging state if $I_{s,t}^{\text{ESS}} = 1$ and discharging state if $I_{s,t}^{\text{ESS}} = 0$. $I_{s,t}^{\text{RT}}$ is also a binary variable, the VPP purchases power at the real-time market if $I_{s,t}^{\text{RT}} = 0$.

The nodal power balance are constrained as (12) and (13). The node voltage range limit constraints are formulated as (14) and (15). The power transmission limit constraints are formulated as (16) and (17). The charging/discharging power limit of energy storage are formulated as (18) and (19). The energy constraints of energy storage are formulated as (20)-(22). The purchased and sold power limit constraints are formulated as (23) and (24). The PV output limits are formulated as (25).

C. Lower Level Boundary Condition Model

1) *Day-ahead market clearing process.* In the day-ahead market, the market operator will clear the market after all the participants have submitted their bid/offers. The market clearing price can be affected by the VPP's quantity bid, especially when the VPP engages in the market as a price-maker. The residual energy curve (REC) is adopted to describe this impact to simplify the market-clearing process [11][12]. Given the VPP's potential participation in the day-ahead market as either an energy producer or a consumer, this paper divides the REC into the residual supply curve (RSC) and the residual demand curve (RDC) to distinguish the roles of VPP within the day-ahead market. The influence of the VPP's bids/offers on the day-ahead market clearing results can be expressed as (26) and (27).

$$\{p_t^{\text{clear,sell}}, P_t^{\text{clear,sell}}\} = F^{\text{RDC}}(p_t^{\text{offer}}, P_t^{\text{offer}}), \forall t \quad (26)$$

$$\{p_t^{\text{clear,buy}}, P_t^{\text{clear,buy}}\} = F^{\text{RSC}}(p_t^{\text{bid}}, P_t^{\text{bid}}), \forall t \quad (27)$$

where $F^{\text{RDC}}(\cdot)$ and $F^{\text{RSC}}(\cdot)$ represent the functional relationships of the impact of VPP's offers as a producer or bids as a consumer on the market clearing results, respectively.

The REC curves can be generally converted from the aggregate total supply curve and aggregate total demand curve disclosed in the market, as illustrated in Fig.4. The market operator forms an initial clearing point based on the bids/offers information of all participants in the market except the VPP, which means that if the VPP's bid/offer is 0, the market clearing price would be p_0 . Furthermore, the VPP can form a series of new clearing points in the market by adjusting its own bids/offers (as a producer, it is equivalent to shifting the supply curve to the right; as a consumer, it is equivalent to shifting the demand curve to the right), then a series of new clearing points constitute the REC curve of the VPP.

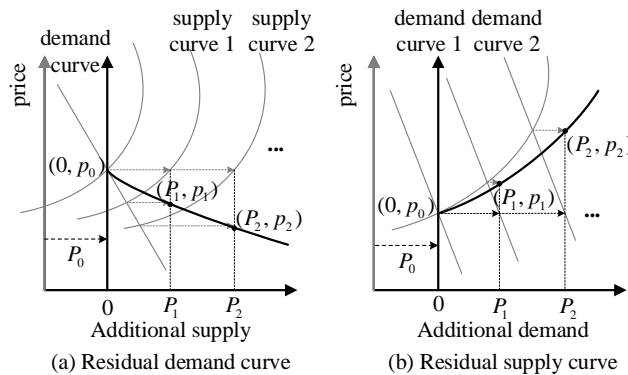


Fig. 4. Translate the supply-demand curves to the residual energy curves.

The REC method can reflect the impact of a price-maker VPP's bids/offers on the day-ahead market clearing results. In most current electricity markets, although market operators would not disclose the specific bidding information of participants, they would usually disclose the day-ahead total supply curve and demand curve [29]. Therefore, the VPP can predict the total supply and demand curves of the next day's market through historical data, and then construct a REC curve to support its day-ahead bid/offer decisions. It is noted that due to the day-ahead market and real-time market are operated separately, we describe the uncertainty of the real-time market price through typical scenarios rather than modeling the real-time market as another lower-level problem.

2) *Demand response model for charging station.* The energy consumption plans of the charging stations are a function of the retail price issued by the VPP, as shown in (10). The charging stations optimize their own charging and discharging power according to the retail price, so as to minimize their own energy cost, the objective function is shown in (28). For a charging station, since the randomness of the number of electric vehicles connected to it at different times, its actual regulated capacity is time-varying. In this paper, the charging stations within the VPP are treated as generalized energy storage devices, with their capacity varying according to the grid-connected status of the electric vehicles [30]. The equivalent power and energy parameters are the Minkowski sum of the corresponding values of all grid-connected electric vehicles at the current moment. It is noted that we ignore the complementary constraint which avoids the simultaneously charge and discharge power of the charging station, which is reasonable under the objective (28).

$$\min_{P_{c,t}^{\text{CS, ch}}, P_{c,t}^{\text{CS, dis}}} \sum_{t=1}^{N_T} P_{t,c}^{\text{ret}} (P_{c,t}^{\text{CS, ch}} - P_{c,t}^{\text{CS, dis}}) \Delta t \quad (28)$$

$$\text{s.t. } 0 \leq P_{c,t}^{\text{CS, ch}} \leq P_{c,t}^{\text{CS, max}} \quad (29)$$

$$0 \leq P_{c,t}^{\text{CS, dis}} \leq P_{c,t}^{\text{CS, max}} \quad (30)$$

$$E_{c,t}^{\text{CS}} = E_{c,t-1}^{\text{CS}} + \Delta E_{c,t}^{\text{CS}} + \eta_c^{\text{CS, ch}} P_{c,t}^{\text{CS, ch}} \Delta t - P_{c,t}^{\text{CS, dis}} \Delta t / \eta_c^{\text{CS, dis}} \quad (31)$$

$$E_{c,t}^{\text{CS, min}} \leq E_{c,t}^{\text{CS}} \leq E_{c,t}^{\text{CS, max}} \quad (32)$$

where $\{P_{c,t}^{\text{CS, max}}, \Delta E_{c,t}^{\text{CS}}, E_{c,t}^{\text{CS, min}}, E_{c,t}^{\text{CS, max}}\}$ are the parameter set of charging station c . $\Delta E_{c,t}^{\text{CS}}$ indicates the variations of the equivalent SOC of charging station c , which can be calculated according to (33).

$$\Delta E_{c,t}^{\text{CS}} = \sum_{n \in \Omega_c^{\text{EV}}} (E_n^a I_{n,t}^{\text{EV}} (I_{n,t}^{\text{EV}} - I_{n,t-1}^{\text{EV}}) - E_n^d I_{n,t-1}^{\text{EV}} (I_{n,t-1}^{\text{EV}} - I_{n,t}^{\text{EV}})) \quad (33)$$

where $I_{n,t}^{\text{EV}}$ is a binary variable and equals to 1 if the EV n is integrated into the grid at time t . E_n^a and E_n^d represent the initial SOC upon the arrival of EV n and the expected SOC at the time of its departure.

D. Abstract Formulation

To enhance notation brevity, the original model are presented using matrices and vectors before introducing the detailed solution methodology and algorithm. Then the distributionally robust model for the VPP can be reformulated as the following compact mathematical representation.

$$\max_{\mathbf{x}_1, \mathbf{x}_2} (\mathbf{A}(\mathbf{x}_1) \mathbf{x}_1 + \sum_{c \in \Omega^{\text{CS}}} \mathbf{x}_2^{\text{T}} \mathbf{z}_c) + \min_{\{\boldsymbol{\pi}\} \in \Psi} \sum_{s=1}^{N_s} \pi_s \max_{\mathbf{y}_s \in Y(\mathbf{x}, \xi_s)} \mathbf{B} \mathbf{y}_s \quad (34)$$

$$\text{s.t. } \mathbf{C} \mathbf{x}_1 \leq \mathbf{c}, \mathbf{H} \mathbf{x}_2 \leq \mathbf{h} \quad (35)$$

$$\mathbf{D} \mathbf{x} + \mathbf{E} \mathbf{y}_s + \sum_{c \in \Omega^{\text{CS}}} \mathbf{F} \mathbf{z}_c = \mathbf{0}, \forall s \quad (36)$$

$$\mathbf{G} \mathbf{y}_s \leq \mathbf{g}, \mathbf{K} \mathbf{y}_s = \mathbf{k}, \forall s \quad (37)$$

$$\mathbf{z}_c = \arg \min_{\mathbf{z}_c \in \mathbf{Z}} (\mathbf{x}_2^*)^{\text{T}} \mathbf{z}_c, \forall c \quad (38)$$

where $\mathbf{x} = [\mathbf{x}_1; \mathbf{x}_2]$, and $\mathbf{x}_1 = [P_t^{\text{bid}}, P_t^{\text{offer}}, I_t^{\text{EM}}]^{\text{T}}$ represents the bidding decisions in day-ahead market with a proper dimension, \mathbf{x}_2 represents the retail price decision $\{P_{t,c}^{\text{ret}}\}$ with a proper dimension. $\mathbf{z}_c = [P_{c,t}^{\text{CS, ch}}, P_{c,t}^{\text{CS, dis}} | \forall c, t]^{\text{T}}$ is the decision variables for charging station c , \mathbf{x}_2^* means it is a given parameter at the lower level demand response model of charging station. ζ_s represents the forecast PV power in scenario s . $\mathbf{A}(\mathbf{x}_1) = [-p_t^{\text{clear, buy}}, p_t^{\text{clear, sell}}, \mathbf{0}]$, means that all the elements are associated with \mathbf{x}_1 . $\mathbf{B} = [p_t^{\text{penalty}} - p_{s,t}^{\text{RT}}, p_t^{\text{penalty}} + p_{s,t}^{\text{RT}}, \mathbf{0}]$. The relationships between the compact constraint

forms and original constraints are shown as (39)-(42). In the practical application, we can use the *export* function in YALMIP to obtain the corresponding coefficient matrix.

$$\mathbf{C}\mathbf{x}_1 \leq \mathbf{c} = \left\{ 0 \leq P_t^{\text{offer}} \leq I_t^{\text{EM}} P_t^{\text{sell,max}}, 0 \leq P_t^{\text{bid}} \leq (1 - I_t^{\text{EM}}) P_t^{\text{buy,max}} \right\}, \mathbf{H}\mathbf{x}_2 \leq \mathbf{h} = \left\{ P_{t,c}^{\text{ret,min}} \leq p_{t,c}^{\text{ret}} \leq P_{t,c}^{\text{ret,max}}, \sum_{t=1}^{N_T} P_{t,c}^{\text{ret}} / N_T \leq p_c^{\text{av}} \right\} \quad (39)$$

$$\begin{aligned} \mathbf{D}\mathbf{x} + \mathbf{E}\mathbf{y}_s + \sum_{c \in \Omega^{\text{CS}}} \mathbf{F}\mathbf{z}_c = 0 = & \{ M_i^{\text{NE}} (P_t^{\text{clear,buy}} - P_t^{\text{clear,sell}}) + \sum_{e \in \Omega^{\text{ESS}}} M_{i,e}^{\text{ESS}} (P_{s,e,t}^{\text{ESS,dis}} - P_{s,e,t}^{\text{ESS,ch}}) + \sum_{r \in \Omega^{\text{RN}}} M_{i,r}^{\text{RN}} P_{s,r,t}^{\text{RN}} + \\ & \sum_{c \in \Omega^{\text{CS}}} M_{i,c}^{\text{CS}} (P_{c,t}^{\text{CS,dis}} - P_{c,t}^{\text{CS,ch}}) - P_{i,t}^{\text{LD}} + M_i^{\text{NE}} (P_{s,t}^{\text{RT,buy}} - P_{s,t}^{\text{RT,sell}}) = \sum_{l \in \Omega_t^{\text{LN}s}} P_{s,l,t}^{\text{LN}} - \sum_{l \in \Omega_t^{\text{LN}e} (P_{s,l,t}^{\text{LN}} - P_{s,l,t}^{\text{LS}}), \\ & M_i^{\text{NE}} Q_{s,t}^{\text{NE}} - Q_{i,t}^{\text{LD}} = \sum_{l \in \Omega_t^{\text{LN}s} Q_{s,l,t}^{\text{LN}} - \sum_{l \in \Omega_t^{\text{LN}e} (Q_{s,l,t}^{\text{LN}} - Q_{s,l,t}^{\text{LS}}), \end{aligned} \quad (40)$$

$$\begin{aligned} V_{s,i,t}^2 - V_{s,j,t}^2 = & 2(R_i P_{s,i,t}^{\text{LN}} + X_i Q_{s,i,t}^{\text{LN}}) - (R_i^2 + X_i^2) ((P_{s,i,t}^{\text{LN}})^2 + (Q_{s,i,t}^{\text{LN}})^2) / V_{s,i,t}^2 \} \\ \mathbf{G}\mathbf{y}_s \leq \mathbf{g} = & \{ V^{\text{min}} \leq V_{s,i,t} \leq V^{\text{max}}, P_{s,i,t}^{\text{LN,min}} \leq P_{s,i,t}^{\text{LN}} \leq P_{s,i,t}^{\text{LN,max}}, Q_{s,i,t}^{\text{LN,min}} \leq Q_{s,i,t}^{\text{LN}} \leq Q_{s,i,t}^{\text{LN,max}}, \\ & 0 \leq P_{s,e,t}^{\text{ESS,ch}} \leq P_e^{\text{ESS,max}} I_{s,t}^{\text{ESS}}, 0 \leq P_{s,e,t}^{\text{ESS,dis}} \leq P_e^{\text{ESS,max}} (1 - I_{s,t}^{\text{ESS}}), E_{\text{min}}^{\text{ESS}} \leq E_{s,e,t}^{\text{ESS}} \leq E_{\text{max}}^{\text{ESS}}, \\ & 0 \leq P_{s,t}^{\text{RT,sell}} \leq P_{\text{RT,max}} I_{s,t}^{\text{RT}}, 0 \leq P_{s,t}^{\text{RT,buy}} \leq P_{\text{RT,max}} (1 - I_{s,t}^{\text{RT}}), 0 \leq P_{s,r,t}^{\text{RN}} \leq P_{s,r,t}^{\text{RN,max}} \} \end{aligned} \quad (41)$$

$$\mathbf{K}\mathbf{y}_s = \mathbf{k} = \{ E_{s,e,t}^{\text{ESS}} = E_{s,e,t-1}^{\text{ESS}} + \eta_e^{\text{ESS,ch}} P_{s,e,t}^{\text{ESS,ch}} \Delta t - P_{s,e,t}^{\text{ESS,dis}} \Delta t / \eta_e^{\text{ESS,dis}}, E_{s,e,1}^{\text{ESS}} = E_{s,e,N_T}^{\text{ESS}} = E_0^{\text{ESS}} \} \quad (42)$$

IV. MODEL REFORMULATION AND SOLUTION ALGORITHM

In this section, the REC curves are firstly discretized to replace market clearing process with linear equations. Then the game model between the VPP and charging stations is transformed into a tractable single-level model based on the strong duality theory. Finally, a customized C&CG algorithm is developed to solve it according to the special structure of the model.

A. Replacing Market Clearing Process with Linear Equations

In this paper, the VPP's participation in the day-ahead market as a price-maker introduces a bilinear term in (5). By introducing the REC curve and discretizing it piecewise, the bilinear term can be tractable [12][31]. For notation brevity, the meanings of the relevant auxiliary variables introduced in the discretization process are shown in Fig.5. The $u_{t,b}^{\text{offer}}$ and $u_{t,b}^{\text{bid}}$ are binary variables, $u_{t,b}^{\text{offer}}=1$ or $u_{t,b}^{\text{bid}}=1$ mean that the VPP's offers as a producer or bids as a consumer fall into segment b at time t .

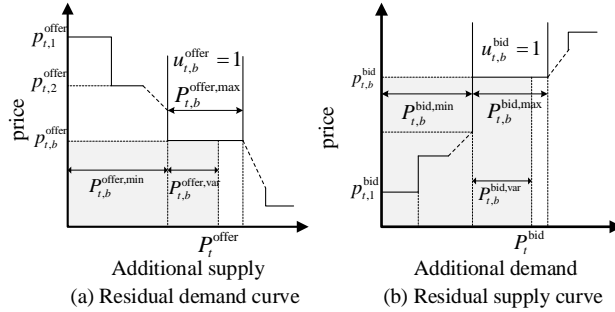


Fig. 5. Linearization process for the residual energy curves.

Based on the discretized REC curves, the VPP's offers as a producer or bids quantity as a consumer can be expressed as the following forms.

$$P_t^{\text{offer}} = \sum_{b=1}^{N_b} (P_{t,b}^{\text{offer,var}} + u_{t,b}^{\text{offer}} P_{t,b}^{\text{offer,min}}) \quad (43)$$

$$0 \leq P_{t,b}^{\text{offer,var}} \leq u_{t,b}^{\text{offer}} P_{t,b}^{\text{offer,max}}, \sum_{b=1}^{N_b} u_{t,b}^{\text{offer}} = I_t^{\text{EM}} \quad (44)$$

$$P_t^{\text{bid}} = \sum_{b=1}^{N_b} (P_{t,b}^{\text{bid,var}} + u_{t,b}^{\text{bid}} P_{t,b}^{\text{bid,min}}) \quad (45)$$

$$0 \leq P_{t,b}^{\text{bid,var}} \leq u_{t,b}^{\text{bid}} P_{t,b}^{\text{bid,max}}, \sum_{b=1}^{N_b} u_{t,b}^{\text{bid}} = 1 - I_t^{\text{EM}} \quad (46)$$

In this paper, the day-ahead market clearing price will be determined by the price-maker VPP's bid quantity and the REC curves.

$$P_t^{\text{clear}} = \sum_{b=1}^{N_b} P_{t,b}^{\text{offer}} u_{t,b}^{\text{offer}} + \sum_{b=1}^{N_b} P_{t,b}^{\text{bid}} u_{t,b}^{\text{bid}} \quad (47)$$

Based on the market clearing electricity price and the characteristics of 0-1 auxiliary variables, the VPP's day-ahead revenue is shown in the shaded part of Fig.5, which can be expressed as the following equations.

$$p_t^{\text{clear,sell}} P_t^{\text{clear,sell}} = p_t^{\text{clear,sell}} P_t^{\text{offer}} = \sum_{b=1}^{N_b} p_{t,b}^{\text{offer}} (P_{t,b}^{\text{offer,var}} + u_{t,b}^{\text{offer}} P_{t,b}^{\text{offer,min}}) \quad (48)$$

$$p_t^{\text{clear,buy}} P_t^{\text{clear,buy}} = p_t^{\text{clear,buy}} P_t^{\text{bid}} = \sum_{b=1}^{N_b} p_{t,b}^{\text{bid}} (P_{t,b}^{\text{bid,var}} + u_{t,b}^{\text{bid}} P_{t,b}^{\text{bid,min}}) \quad (49)$$

B. Demand response problem transformation

A Stackelberg game is formulated between the charging stations and the VPP. The VPP is the leader and the charging stations are the followers. When the retail price issued by the VPP is given, the demand response model of the charging stations is transformed into a linear programming, and its compact form is shown as follows.

$$\begin{aligned} & \min_{z_c} (\mathbf{x}_2^*)^T z_c \\ & \text{s.t. } \mathbf{M}_c z_c = \mathbf{m}_c : \alpha_c \\ & \quad \mathbf{Q}_c z_c \leq \mathbf{q}_c : \beta_c \end{aligned} \quad (50)$$

where α_c and β_c are the dual variables of corresponding constraints.

The game model can be transformed based on the KKT condition or the primal-dual method. In this paper, the KKT conditions method is adopted to tackle the bi-level model. The solution of the following equations are the optimal solution of the demand response model of the charging station.

$$(\mathbf{x}_2^*)^T + \beta_c^T \mathbf{Q}_c + \alpha_c^T \mathbf{M}_c = 0 \quad (51)$$

$$\text{diag}(\beta_c) \cdot (\mathbf{Q}_c z_c - \mathbf{q}_c) = 0 \quad (52)$$

$$\beta_c \geq 0 \quad (53)$$

Among them, Eq. (52) can be further converted into the following form based on the big-M method.

$$\mathbf{M}(\mathbf{I}_c^{\text{BM}} - \mathbf{1}) \leq \mathbf{Q}_c z_c - \mathbf{q}_c \leq \mathbf{0} \quad (54)$$

$$\mathbf{0} \leq \beta_c \leq \mathbf{M} \mathbf{I}_c^{\text{BM}} \quad (55)$$

where \mathbf{I}_c^{BM} is an ancillary binary variable. M denotes a large enough number and Ref. [32] provides guidance on selecting an appropriate value for M.

In addition, since the retail price is a decision variable in the first-stage optimization model of the VPP, the second term in (34) is nonlinear. Based on the KKT complementary slackness conditions and the strong duality theory, the bilinear term can be converted into the following linear form by multiplying z_c on both sides of (51).

$$\sum_{c \in \Omega^{\text{cs}}} \mathbf{x}_2^T z_c = - \sum_{c \in \Omega^{\text{cs}}} (\mathbf{q}_c^T \beta_c + \mathbf{m}_c^T \alpha_c) \quad (56)$$

where \mathbf{q}_c and \mathbf{m}_c are both the given parameters, thus the nonlinear term $\sum_{c \in \Omega^{\text{cs}}} \mathbf{x}_2^T z_c$ in (34) can be transformed into a linear combinations of dual variables.

C. The iterative decomposition algorithm

The objective function (34) processed by Section IV-A and Section IV-B can be transformed into the following two-stage max-min-max optimization form. Notably, this form cannot be directly solvable using currently available commercial solvers.

$$\max_{x_1, x_2, \alpha_c, \beta_c} (\mathbf{A}x_1 - \sum_{c \in \Omega^{\text{cs}}} (\mathbf{q}_c^T \beta_c + \mathbf{m}_c^T \alpha_c)) + \min_{\{\boldsymbol{\pi}\} \in \Psi} \sum_{s=1}^{N_s} \pi_s \max_{y_s \in Y(x, \boldsymbol{\pi}_s)} \mathbf{B}y_s \quad (57)$$

Theoretically, the above model can be addressed using either the Benders-dual cutting plane method or the C&CG algorithm. Notably, the C&CG algorithm stands out for its simplicity and superior convergence performance when

compared with the former one [33]. More specifically, the conventional C&CG algorithm solves the aforementioned robust model by dividing it into a master problem (MP) and a sub-problem (SP). Furthermore, it transforms the second-stage min-max optimization problem into a single level model based on the duality theory. However, in this paper, since the model contains 0-1 variables that depict the charging state of the energy storage and electricity purchase status of the VPP, the duality theory cannot be directly applied, and a more complex nested-C&CG algorithm needs to be adopted [34], which seriously affects the solution efficiency. Therefore, we developed a customized C&CG algorithm according to the special structure of the robust model, and there is no need for primal-dual transformation of subproblems. By further decomposing the sub-problems into several small-scale linear programming problems that are independent of each other, we can use the parallel computing to speed up the solution efficiency.

The master problem is as follows.

$$\text{MP: } \max_{x_1, x_2, a_c, \beta_c, \eta} (\mathbf{A}x_1 - \sum_{c \in \Omega^{\text{CS}}} (q_c^T \beta_c + m_c^T a_c)) + \eta \quad (58.1)$$

$$\text{s.t. } (51), (53) - (55) \quad (58.2)$$

$$\mathbf{C}x_1 \leq c, \mathbf{H}x_2 \leq h \quad (58.3)$$

$$\eta \leq \sum_{s=1}^{N_s} \pi_{s,*}^{(k)} \max_{y_s^{(k)} \in Y(x, \xi_s)} \mathbf{B}y_s^{(k)}, \forall k = 1, \dots, K \quad (58.4)$$

$$\mathbf{G}y_s^{(k)} \leq \mathbf{g}, \mathbf{K}y_s^{(k)} = \mathbf{k}, \forall s, \forall k = 1, \dots, K \quad (58.5)$$

$$\mathbf{D}x + \mathbf{E}y_s^{(k)} + \sum_{c \in \Omega^{\text{CS}}} \mathbf{F}z_c = 0, \forall s, \forall k = 1, \dots, K \quad (58.6)$$

where η is the objective function value of the sub-problem. $y_s^{(k)}$ is the decision variable vector for the k -th iteration in scenario s . $\pi_{s,*}^{(k)}$ is the worst case of probability distribution realization for the k -th iteration obtained from the sub-problem.

The sub-problem is as follows.

$$\text{SP: } F(\mathbf{x}^*) = \min_{\{\pi\} \in \Psi} \sum_{s=1}^{N_s} \pi_s \max_{y_s \in Y(x^*, \xi_s)} \mathbf{B}y_s \quad (59.1)$$

$$\text{s.t. } \mathbf{G}y_s \leq \mathbf{g}, \mathbf{K}y_s = \mathbf{k}, \forall s \quad (59.2)$$

$$\mathbf{D}x^* + \mathbf{E}y_s + \sum_{c \in \Omega^{\text{CS}}} \mathbf{F}z_c = 0, \forall s \quad (59.3)$$

Since the decision variables between different scenarios are independent of each other in the aforementioned sub-problem, it can be split into an inner-level problem and an outer-level problem to be solved independently, as shown follows.

$$f(\mathbf{x}^*) = \{ \max_{y_s \in Y(x^*, \xi_s)} \mathbf{B}y_s : \text{s.t. } (59.2) - (59.3) \} \quad (60)$$

$$F(\mathbf{x}^*) = \min_{\{\pi\} \in \Psi} \sum_{s=1}^{N_s} \pi_s f(\mathbf{x}^*) \quad (61)$$

In summary, the model solving steps can be summarized as follows: given the worst case of probability distribution realization obtained from the sub-problem, the master problem decides the day-ahead offering strategy and retail electricity price issued to end-users so as to maximize its revenue. Subsequently, the sub-problem generates the worst-case probability distribution realization based on the results of the master problem, taking into account the internal security constraints of VPP and the optimal energy storage schedule. The specific solution progress of the algorithm is as follows.

Algorithm 1: Customized C&CG Algorithm.

1. **Set** $LB = -\infty$, $UB = +\infty$, $k=1$, $\varepsilon=0.01$;
 2. **for** $k=1$: k_{\max} , **do**
 3. **Solve** the master problem (58), derive the optimal solution $(\mathbf{x}_k^*, \mathbf{y}_k^*, \mathbf{y}_{s,*}^{(k)})$, namely the optimal day-ahead bidding strategies in the market and the released retail price, update $UB = \min\{UB, \mathbf{A}\mathbf{x}_k^* + \eta_k^*\}$.
 4. **Parallel solve** the inner-level of the sub-problem (60), derive the optimal decisions y_s of the second stage under each scenario s .
 5. **Solve** the outer-level of the sub-problem (61), derive the worst case of probability distribution realizations of PV output $\pi_{s,*}^{(k)}$, update $LB = \max\{LB, \mathbf{A}\mathbf{x}_k^* + F(\mathbf{x}_k^*)\}$.
-

6. **if** $UB-LB \leq \varepsilon$, then
7. **return** x_k^* and terminate.
8. **else**
9. **Add** the constraints (58.4)-(58.6) to the master problem and go to step 3.
10. **end if**
11. **end for**
12. **Output** the optimal results.

V. CASE STUDIES

The effectiveness of the proposed strategy is verified based on the IEEE 33-node distribution network. The VPP entity engages in the power market through the PCC and should also be responsible for its power network security. In the VPP test system, four PV stations ($4 \times 1.5\text{MW}$) are located at bus #15, #19, #23 and #31, three EVCSs are located at bus #8, #16 and #25, two ESSs ($1.5\text{MW}/3\text{MWh}$) are located at bus #4 and #12. The total adjustable generation capacities are intentionally configured to exceed the fixed load demand to ensure the VPP's capability to act as a prosumer. According to the LHS and scenario reduction methods, 10 scenarios of PV output and real-time market price are generated at first, and the empirical probability distribution of scenarios is shown as Fig.6. The electric vehicles in each charging station are categorized into three types, each associated with specific parameters detailed in TABLE 1. Here, $N(\mu, \sigma)$ denotes a normal distribution with a mean value μ and a standard deviation value σ , $U(a, b)$ denotes a uniform distribution within the range (a, b) . The quantity of electric vehicles integrated into each charging station per day is determined through uniform sampling. The residual energy curves can refer to [12] and the volumes are scaled to make them suitable for the VPP in this paper. All simulations are conducted on a laptop with a 2.1GHz AMD Ryzen 5 4600U CPU and 16 GB RAM. ε is set to be 10^{-6} in the case study.

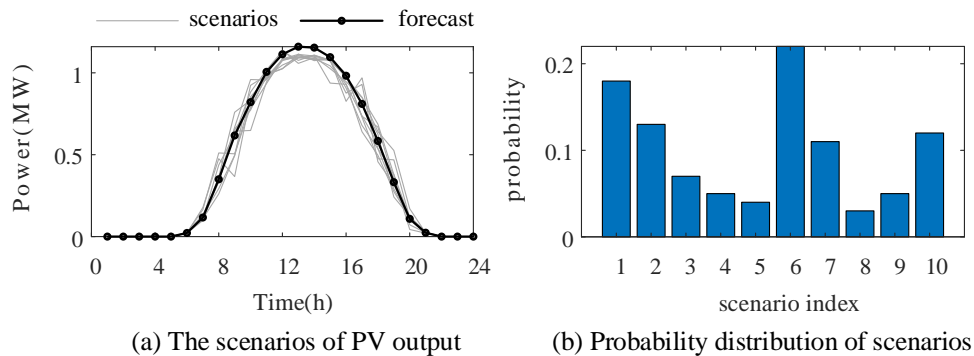


Fig. 6. The input data of PV.

TABLE 1 Parameters for Various Types of Electric Vehicles

Types of EV	Arrival time T_c^a (h)	Departure time T_c^d (h)	Initial SOC
I	$N(9,1)$	$N(17,1)$	$U(0.4,0.6)$
II	$N(0,1)$	$N(9,1)$	$U(0.4,0.6)$
III	$N(17,1)$	$N(25,1)$	$U(0.4,0.6)$

A. Robust offering and pricing results: a demonstrative case

To verify the effectiveness of the robust offering and pricing optimization model, a confidence level of 0.9 is selected for the probability distribution deviation and additional 100 scenarios are generated. Fig.7(a) and (b) show the day-ahead market offering results of the VPP and the internal power balance allocation results. Whether the VPP offers as a producer or bids as a consumer in the day-ahead market depends on the REC curves and internal supply and demand conditions. In Fig.7(a), the green line represents the original cleared electricity price when the VPP does not participate in the day-ahead market, and the yellow line represents the cleared electricity price after the VPP participates in the market as a price-maker. During periods when the day-ahead cleared electricity price is high and there is an excess of electricity within the VPP, the VPP typically tends to engage in the day-ahead market as a producer. For instance, from 11:00 to 12:00, the VPP's participation as a producer increases the market supply, resulting in a reduction in the cleared electricity price. Similarly, when the day-ahead electricity price is low and the VPP's internal load demand is

substantial, the VPP will engage in the day-ahead market as a consumer. For example, during the period from 5:00 to 8:00, the increase in electric energy demand in the market further contributes to the increase of cleared electricity price. The analyses above reflect the impact of the price-maker VPP on the market clearing price, which is beneficial for the VPP to flexibly switch between a producer and a consumer and adopt a reasonable offering strategy to maximize its own benefits. This can be further verified in Fig.7(b). In Fig.7(b), the red curve represents the VPP's net power purchase curve, depicting the difference between the VPP's power purchase in the real-time market and the day-ahead market. At night (such as 2:00-6:00), when there is no PV output and the load demand is high, the VPP must purchase a large amount of electricity to fulfill the internal load demand. Conversely, when the PV output is abundant around noon (such as 11:00-12:00), the VPP has the opportunity to sell surplus electricity in the real-time market to make a profit after satisfying the internal energy demand.

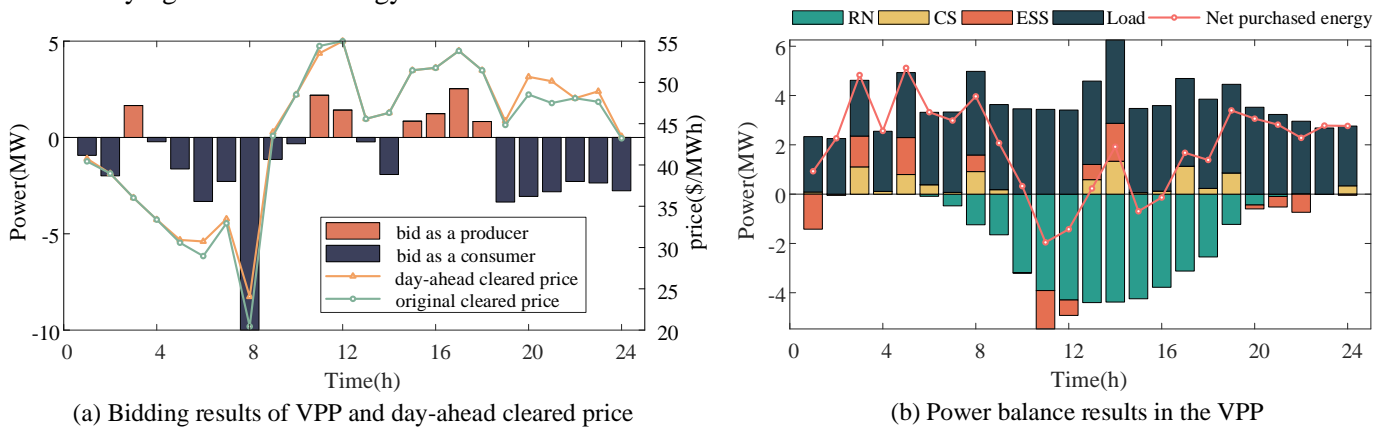


Fig. 7. Bidding results of VPP and power balance results.

The VPP's purchased power for a specific scenario is demonstrated in Fig. 8. As can be seen from Fig.8(a)-(b), the VPP has the following two behaviors at the same time, engaging in the electricity purchase of in the day-ahead market and the electricity sale in the real-time market. When the day-ahead market electricity price is higher than that in the real-time market (such as 15:00-18:00), the VPP is more inclined to sell electricity in the day-ahead market and buy electricity in the real-time market to complete the day-ahead energy contract. Fig.8(c)-(d) show the pricing results within the VPP and the demand response behaviors of each charging station under the retail electricity price. Due to the different types and parameters of electric vehicles in each charging station, coupled with the considerations of the power flow constraints within the VPP, the charging stations connected to different nodes have varying effects on the VPP's operation benefits, so the VPP gives different pricing results for individual charging stations. The distributed PV output and the node voltage at each time in a certain scenario are shown in Fig.9. Since the strategy presented in this paper accounts for voltage constraints within the VPP, even during periods of high PV output, such as around noon (e.g. 11:00-12:00), the voltage of each node can be maintained at a reasonable level, which greatly ensures the VPP's operation safety.

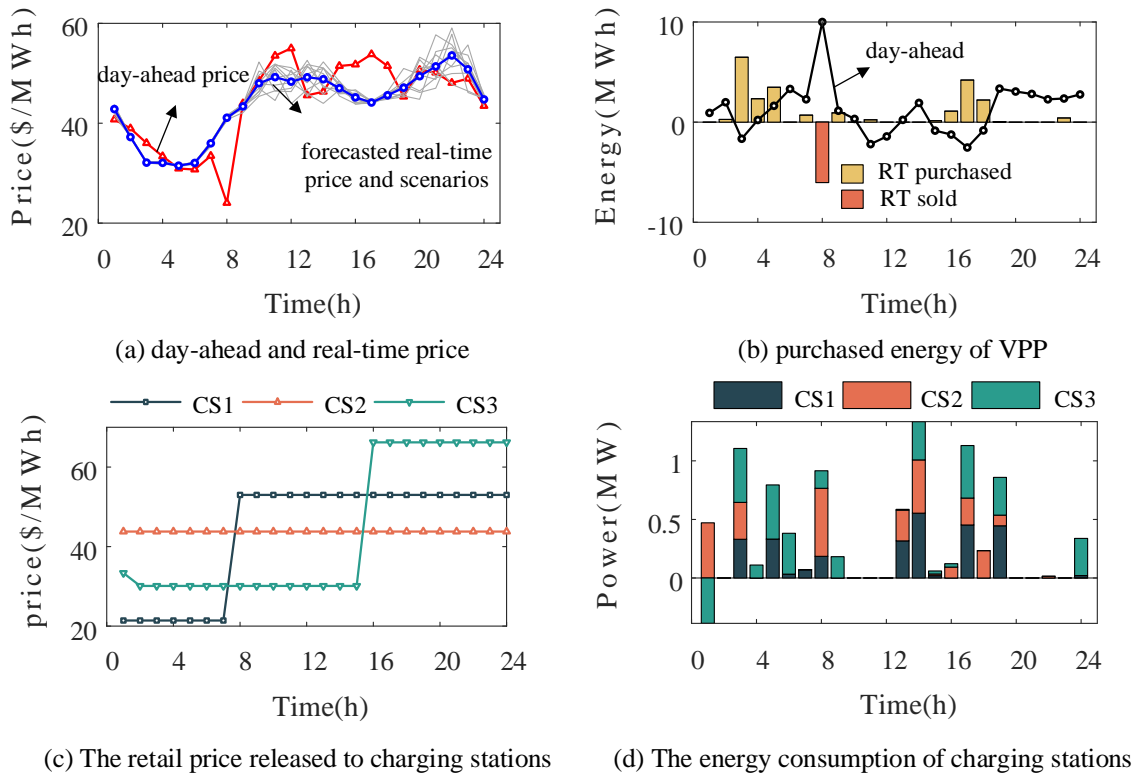


Fig. 8. The first-stage and second-stage (at a specific scenario) optimization results.

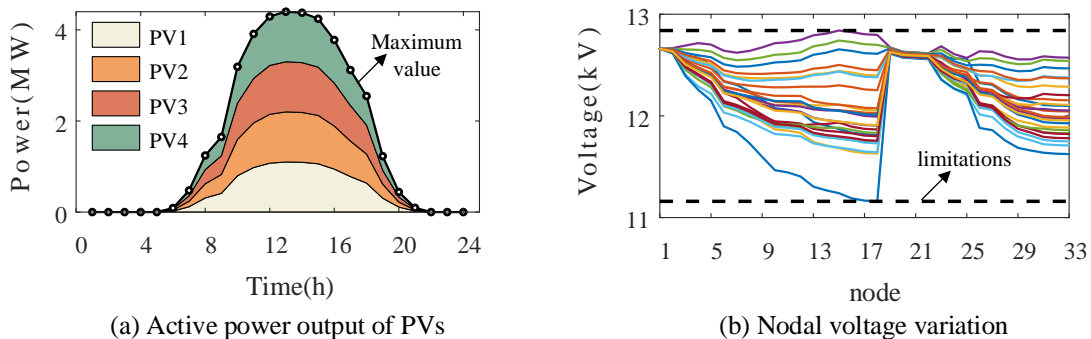


Fig. 9. The active power output of PVs (at a specific scenario) and the corresponding effects of proposed strategy.

Fig.10 shows the comparison of the results under the worst-case probability distribution and empirical distribution of the distributed PV forecast errors. It can be seen from Fig.10 that under different probability distributions of PV forecast errors, the VPP's day-ahead offers are almost the same. This is because the VPP has flexible adjustment equipment such as energy storage that can adapt to the user's power demand, so the VPP will not significantly adjust its day-ahead offering decisions resulting from the uncertainty of the PV forecast errors. On the contrary, it is more inclined to balance the power deviation through energy storage after getting the user's actual energy demand response. The detailed analysis of the energy storage's impact on the VPP's decision-making will be illustrated in the Section V-D. TABLE 2 shows the various costs of the VPP under the empirical distribution and the worst-case probability distribution realizations. The VPP's total energy cost under the worst-case probability distribution realizations only increased by 0.8% compared with the empirical distribution. This observation pertains to the quantity of scenarios employed in this section. By generating a substantial number of scenarios, the worst-case probability distribution realizations tend to align more closely with the empirical distribution, thus preventing any economic losses stemming from overly conservative decision-making results.

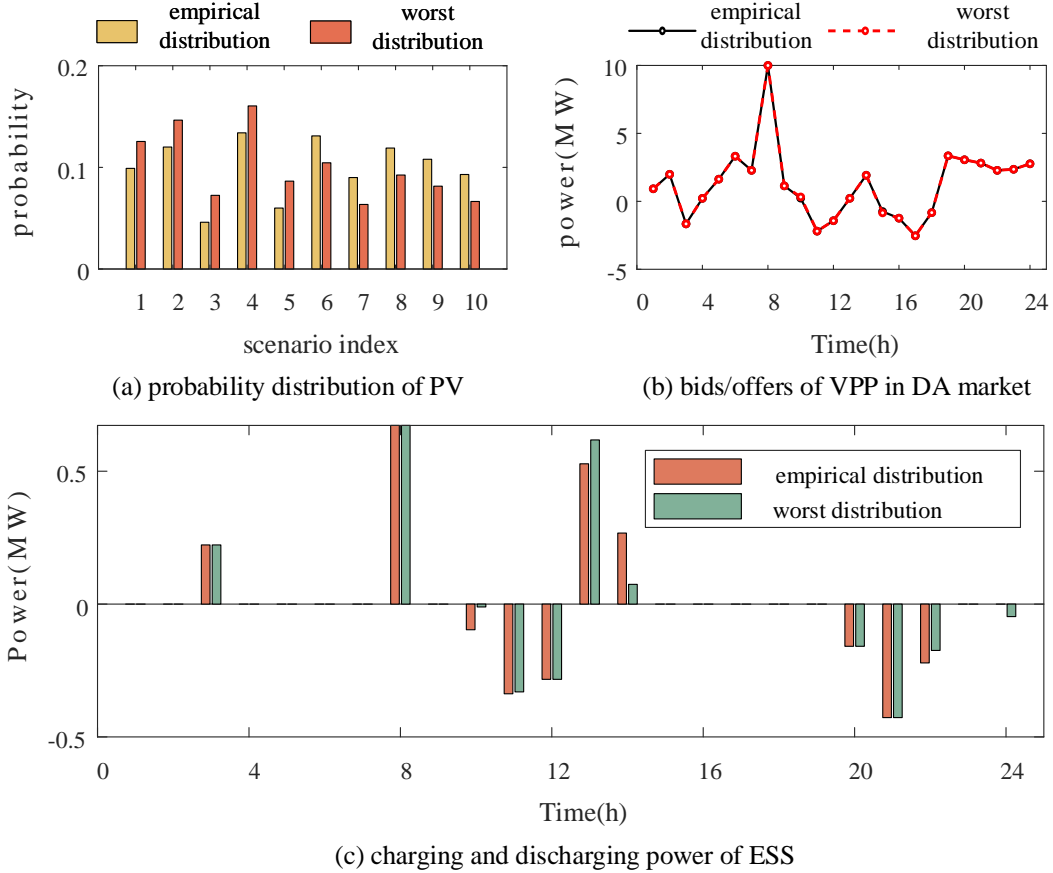


Fig.10. The optimization results of different probability distribution of PV.

TABLE 2 Cost of VPP under different probability distribution of PV

Cost/Revenue(\$)	Empirical distribution	Worst distribution
day-ahead purchased cost	1547.80	1552.00
day-ahead sold revenue	536.67	541.77
revenue from CSs	366.39	366.39
real-time purchased cost	835.99	845.55
real-time sold revenue	276.11	274.92
penalty due to deviation	111.21	112.05
Total cost	1315.83	1326.52

B. Comparison of price-maker and price-taker strategies

In this section, the proposed strategy (Scheme 1) is compared with the following schemes.

Scheme 2 (price-taker): VPP engages in the day-ahead market as a price-taker, which means the VPP's bids on the market clearing price is not considered. The model for a price-taker strategy of VPP is as follows. The rest of the settings remain the same as in Scheme 1.

$$\max_x \Delta t \sum_{t=1}^{N_T} (p_t^{\text{DA}} P_t^{\text{DA}} + \sum_{c=1}^{N_{CS}} p_{t,c}^{\text{ret}} (P_{c,t}^{\text{CS,ch}} - P_{c,t}^{\text{CS,dis}})) \quad (62a)$$

$$\text{s.t.} \quad p_{t,c}^{\text{ret,min}} \leq p_{t,c}^{\text{ret}} \leq p_{t,c}^{\text{ret,max}}, \forall t, c \quad (62b)$$

$$\sum_{t=1}^{N_T} p_{t,c}^{\text{ret}} / N_T \leq p_c^{\text{av}}, \forall c \quad (62c)$$

$$-P_t^{\text{max}} \leq P_t^{\text{DA}} \leq P_t^{\text{max}}, \forall t \quad (62d)$$

$$\{P_{c,t}^{\text{CS,ch}}, P_{c,t}^{\text{CS,dis}}\} = F_n^{\text{EVCS}}(p_{t,c}^{\text{ret}}), \forall t, c \quad (62e)$$

$$(11) - (25) \quad (62f)$$

TABLE 3 Cost of VPP participating as a price-maker or a price-taker

Cost/Revenue(\$)	Price-maker	Price-taker
day-ahead purchased cost	1552.00	3834.05
day-ahead sold revenue	541.77	2244.87
revenue from CSs	366.39	364.33
real-time purchased cost	845.55	2538.29
real-time sold revenue	274.92	1388.10
penalty	112.05	392.64
Total cost	1326.52	2767.68

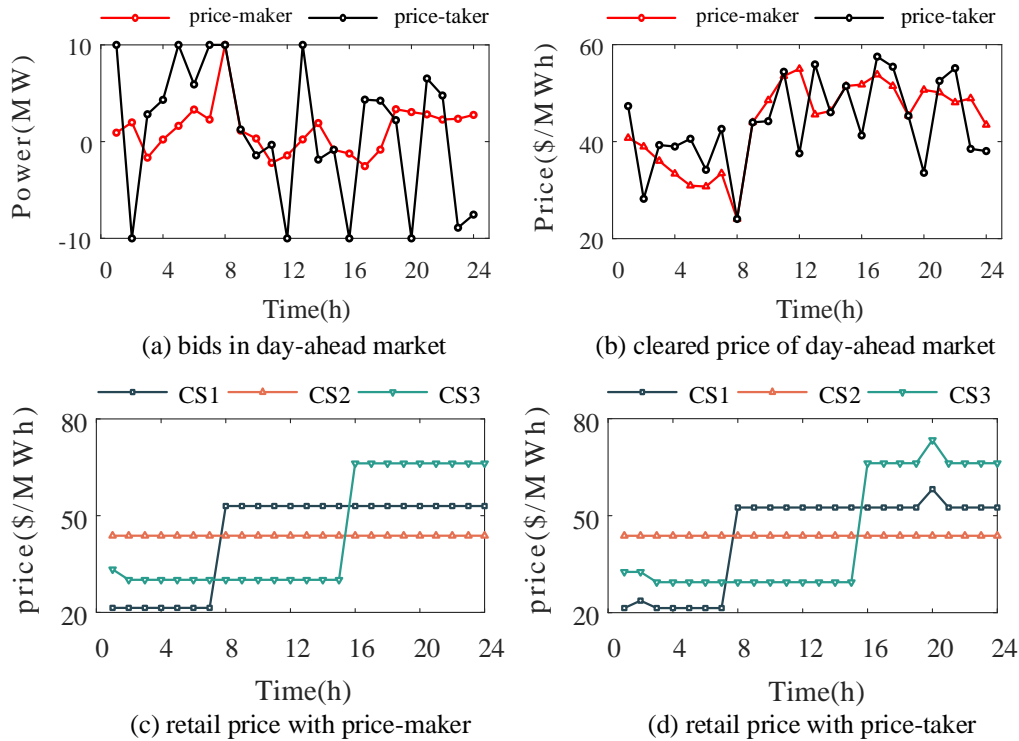


Fig.11. Comparisons with VPP participating as a price maker or a price taker.

TABLE 3 shows the energy cost of the VPP under different schemes. Notably, when the VPP takes on the role of a price-maker in the day-ahead market, it incurs lower energy cost compared to its position as a price-taker. Further, the day-ahead power purchased curves of the VPP under different schemes are shown in Fig.11 (a) and the day-ahead market clearing price is shown in Fig.11(b). Compared with Scheme1, the power purchased curves of the VPP under Scheme 2 is more extreme and always touches the boundary of the offering. In Fig.11(b), The black curve represents the day-ahead cleared electricity price, accounting for the impact of VPP's role as a price-taker on the clearing price. From Fig.11(a) and (b), we can see that when the VPP engages in the day-ahead market as a consumer (such as 4:00-8:00), the market clearing price under Scheme 2 is higher than Scheme 1, and when the VPP engages in the day-ahead market as a producer, the cleared electricity price under Scheme 2 will be lower than Scheme 1. In other words, the price-maker VPP is more inclined to sell electricity during periods of high prices and purchase electricity during periods of low prices. Compared with price-takers, they can make more reasonable day-ahead decisions and thus have more arbitrage opportunities.

Fig.11 (c) and (d) show the pricing results of the VPP under Scheme 1 and Scheme 2, respectively. At $t=2$ and $t=20$, the retail price released to electric vehicle charging stations under Scheme 2 is higher than that under Scheme 1. This is because VPP's day-ahead electricity offers are too large at this time under Scheme 2, and the distributed PV output is low at the same time, so VPP needs to issue a higher retail price to encourage EVCSs to discharge so as to reduce the deviation from the day-ahead contract as much as possible. These results further validate the necessity of coordinated offering and pricing strategy proposed in this paper when a price-maker VPP participates in the day-ahead

market.

C. Comparison of different uncertainty models

In this section, the strategy proposed in this paper is compared with the following schemes to verify the advantage that both economy and conservatism can be considered when dealing with the uncertainties.

Scheme 3: the traditional robust optimization strategy is adopted, in which the budget uncertainty set is used to describe the photovoltaic output uncertainty [35], the boundary prediction deviation of the uncertainty set is set to 0.1 of the predicted value, and the budget is set to 24.

Scheme 4: a two-stage stochastic optimization strategy is employed to model the problem, involving the generation of 1000 PV output scenarios. The decision variables in each stage are the same as those in Scheme 1.

TABLE 4 Cost of virtual power plant under different schemes

Cost/Revenue(\$)	Scheme 1	Scheme 3	Scheme 4	
			expected value	worst scenario
day-ahead purchased cost	1552.00	1574.26	1547.80	1547.80
day-ahead sold revenue	541.77	510.26	534.92	534.92
revenue from CSs	366.39	366.39	366.39	366.39
real-time purchased cost	845.55	897.58	834.39	882.26
real-time sold revenue	274.92	259.01	276.11	245.84
penalty	112.05	115.66	111.05	112.81
Total cost	1326.52	1451.84	1315.82	1395.72

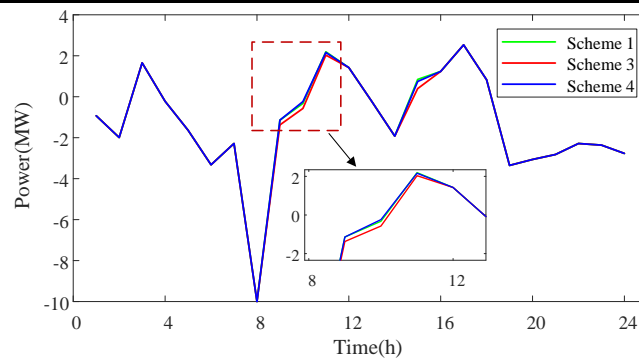


Fig.12. The bids/offers of VPP in day-ahead market under different schemes.

The various costs of the VPP under different schemes are shown in TABLE 4, and the day-ahead offering results is shown in Fig.12. The VPP's total operation cost under the strategy proposed in this paper is between Scheme 3 and Scheme 4, which is lower than Scheme 3 using the traditional robust optimization strategy, and higher than Scheme 4 using two-stage stochastic optimization. Specifically, compared with Scheme 3, the proposed strategy considers the influence of the worst probability distribution realizations of PV prediction errors on the VPP's decision-making, and overcomes the shortcomings that are too conservative in Scheme 3 (the Scheme 3 minimizes the total operating cost under the worst PV output). Therefore, the VPP's total cost in Scheme 1 decreased. Compared with Scheme 4, the two-stage stochastic optimization strategy is based on the assumption that the PV forecast error obeys a specific probability distribution. It does not account for the influence of the worst-case probability distribution realizations of the uncertainty on the VPP's decision-making. Consequently, the expected total cost is lower than that in Scheme 1. However, the VPP's total operating cost in the worst scenario of Scheme 4 is higher than that of Scheme 1, indicating that the strategy optimized by Scheme 1 can adapt to more actual scenarios, and has better economy and robustness than the two-stage stochastic optimization under the worst scenario.

D. Sensitivity analysis

1) *The impact of historical data sizes M .* This section tests the effects of the number of historical scenarios (means the M value before scenario reduction) on the VPP's total cost. Other parameters are consistent with those in Scheme 1 except for the number of scenarios. The comparison of the Scheme1 with the Scheme 3 and Scheme 4 under different

number of historical scenarios is shown in Fig.13. As the number of historical scenarios increases, the allowable deviation limit of the probability distribution of the PV output decreases, so that the worst case of probability distribution realization is closer to the actual probability distribution. The reduced conservativeness of decision-making makes the total energy cost of the VPP also decrease. Besides, the energy cost of the VPP in Scheme 1 is between Scheme 3 and Scheme 4. The energy cost of the VPP under the distributionally robust optimization model approaches the stochastic optimization with the increase of the number of historical scenarios. The computation time for various schemes across different number of historical scenarios are displayed in TABLE 5. In Scheme 1, as the value of M is only related to the bounds of uncertainty set, that is, it affects the size of feasible region, the computation time increases slightly when M increases. Since the number of decision variables and constraints in the traditional robust optimization model of Scheme 3 remains independent of the number of historical scenarios, the solution time remains the same regardless of the scenario count. But they are all higher than Scheme 1, this is because the sub-problems are decomposed into linear programming problems that are independent of each other and solved separately according to the special model structure in this paper, so that there is no need for primal-dual transformation of the sub-problems. In Scheme 4, the number of decision variables and constraints in the second stage is closely related to the number of historical scenarios, resulting an increase in the solution time as the number of historical scenarios increases. The analyses above show that the distributionally robust optimization method adopted in this paper can be both robust and economic by selecting a reasonable number of historical scenarios, and the solution algorithm designed by using the special structure of the model can also have good computational efficiency.

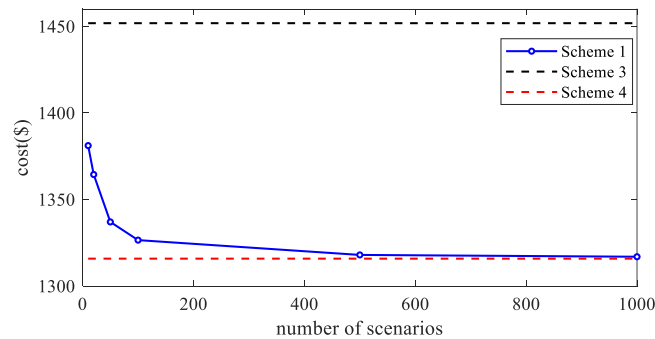


Fig.13. The total cost of three models at different number of historical scenarios.

TABLE 5 Solution time of three models at different number of historical scenarios (s)

Historical scenario sizes M	Scheme 1	Scheme 3	Scheme 4
10	143.52	609.07	35.13
20	131.46	609.07	43.19
50	122.48	609.07	117.91
100	141.14	609.07	249.16
500	225.90	609.07	>1000
1000	321.54	609.07	>1000

2) *The impact of the parameters of ESS.* This section analyzes the impact of energy storage's parameters (initial SOC, power and energy capacity) on the VPP's operation cost, and other parameters are also consistent with those in Scheme 1. Fig.14 shows the impact of whether to configure energy storage within the VPP on its first-stage decision-making, and TABLE 6 gives the operating cost of the VPP under different initial SOC. In the situation where no energy storage is configured within the VPP, the day-ahead offers tend to be more conservative compared to the instance where energy storage is configured within the VPP. The initial SOC of energy storage also has a great effect on the VPP's operation cost. The VPP's operation cost gradually increases with the rise in the initial SOC of energy storage. Therefore, this paper further introduces the initial SOC of energy storage as part of the decision variables in the first stage. As a result, the optimal SOC value for energy storage in this paper is determined to be 0.45MWh. Compared with the SOC value of energy storage which is set at 2.0 MWh in Scheme 1 (i.e., the column 6 in TABLE 6), the operating cost of the VPP decreases from \$1326.52 to \$1297.34. This highlights the significance of selecting an appropriate initial SOC value for energy storage to reduce the operating cost of the VPP. Furthermore, we fix the initial SOC of energy storages as 0.45 and analyze the impact of storage flexibility (power and energy capacity). Fig.15 shows how the VPP's total

operation cost changes with the different energy storage's capacity and maximum power. With the increase of the energy storage's capacity, the VPP's total operation cost decreases. As a contrast, when the maximum power of the energy storage reaches 1MW, the VPP's total operation cost does not change significantly with the increase of the energy storage's maximum power.

TABLE 6 The VPP's operation cost with different initial energy storages' SOC (\$)

Initial SOC	0.45	0.5	1.0	1.5	2.0
Total cost	1297.34	1297.96	1305.26	1316.08	1326.52

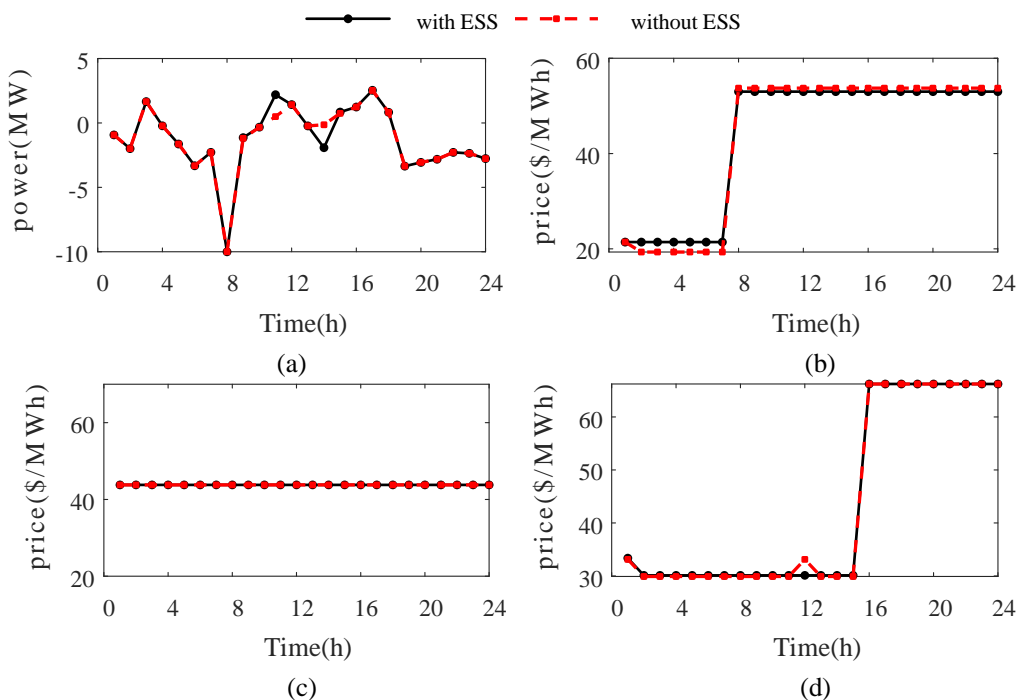


Fig.14. Comparisons of the first-stage decision results: (a) bids/offers of the VPP in day-ahead market. (b) retail price released to CS1. (c) retail price released to CS2. (d) retail price released to CS3.

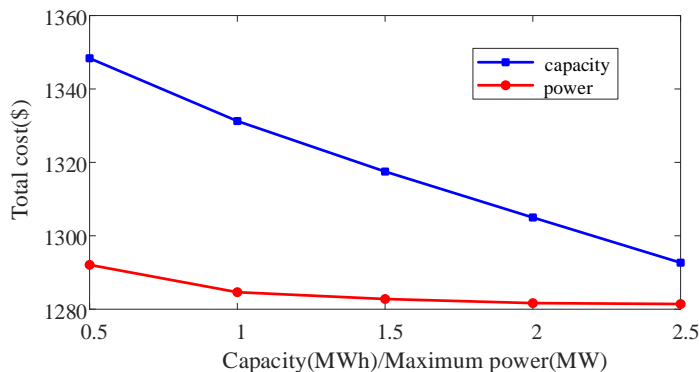


Fig.15. The VPP's total operation cost under different energy storage's capacity and maximum power

3) *The impact of the penalty coefficient p_t^{penalty} .* This section focuses on the impact of the penalty coefficient on the VPP's operation cost. We define the ratio $r = p_t^{\text{penalty}}/p_t^{\text{RT}}$, where p_t^{RT} is the forecasted real-time market price. TABLE 7 shows the VPP's operation cost under different ratio values. With the increase of the penalty cost coefficient, the VPP's day-ahead purchased power cost increases and day-ahead sold power revenue decreases. Meanwhile, in the real-time market, its expected purchased power cost and sold power revenue both decrease significantly, and the total operation cost increases slightly. This is because there are more arbitrage chances for the VPP to maximize its benefit under a small penalty cost coefficient. Therefore, for the market operator, an appropriate deviation punishment

mechanism can avoid the VPP's arbitrage behaviors in the day-ahead market and real-time market, thus promoting the benign development of the market.

TABLE 7 The VPP's operation cost under different ratio values (\$)

ratio	day-ahead purchased cost	day-ahead sold revenue	revenue from CSs	real-time purchased cost	real-time sold revenue	penalty	Total cost
0.01	1316.95	1382.22	365.47	2331.92	802.85	31.35	1129.68
0.03	1359.02	1381.92	365.12	2100.13	605.56	81.17	1187.73
0.05	1342.06	1117.77	364.58	1738.26	471.86	110.51	1236.61
0.07	1367.87	860.64	365.72	1378.22	367.21	122.18	1274.71
0.09	1477.81	718.52	365.54	1106.49	323.62	128.71	1305.33

E. Computational performance

This section conducts experiments to test the computational performance of the iterative algorithm. The confidence level (α_1 and α_∞) is set as 0.9 and the convergence tolerance of the algorithm is set as 10^{-6} . Besides, the Parallel Computing Toolbox in MATLAB is used to perform parallel computations. The number of parallel threads in MATLAB is set to 1, 3 or 6. The computational performance under different number of scenarios and different number of threads are shown as TABLE 8. Fig.16 shows the comparison of the solution time with different number of parallel threads.

From the TABLE 8, we can see that the calculating time of the algorithm increases fast with the increase of the number of scenarios, but they can all converge within 3 iterations. Taking the sixth row in TABLE 8 as an example (the number of scenarios equals 80), the convergence process of the upper and lower bound of the algorithm is shown in TABLE 9. Besides, we can see that the calculation time can be reduced by about 50% by using 3 parallel threads or by about 70% using 6 parallel threads when the number of scenarios is large (such as 60 and 80). The more the number of scenarios, the greater the advantages of parallel computing.

TABLE 8 Computation performance under different number of scenarios and different number of threads

Number of scenarios N_s	Confidence level	Optimal value	Calculating time (s)			Number of iterations
			1 thread	3 threads	6 threads	
10	0.9	1326.52	141.14	45.42	40.64	2
20	0.9	1340.18	516.16	220.53	185.86	3
40	0.9	1359.49	925.95	281.59	255.16	3
60	0.9	1376.01	2949.67	1407.67	1078.89	3
80	0.9	1393.35	5009.52	2921.65	1407.67	3

TABLE 9 The convergence process of the upper and lower bound

Iteration index	Upper bound	Lower bound	Gap (%)
1	-1304.07	-1393.80	6.8800
2	-1393.24	-1393.35	0.0081
3	-1393.35	-1393.35	0.0000

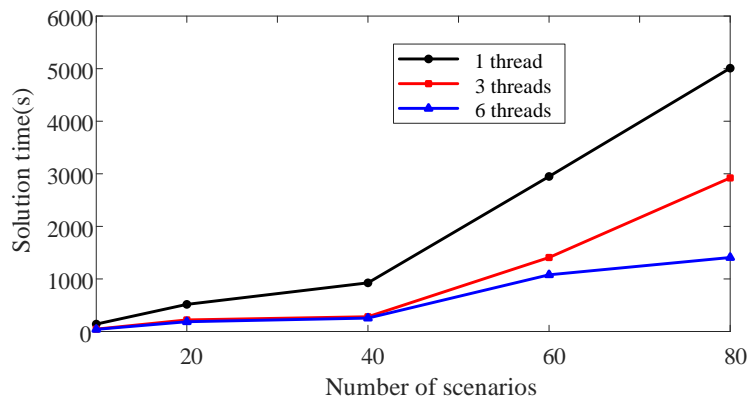


Fig.16. Comparison of the calculating time with different number of parallel threads

VI. CONCLUSION

This paper comprehensively addresses the bids/offers and retail price decision-making problem for a price-maker VPP in the day-ahead market. A two-stage bi-level distributionally robust optimization model is established with a form of max-min-max accordingly and this model can integrate optimization strategies in the real-time market into the day-ahead optimization, which helps ensure the safe operation of the VPP and the optimality of the VPP's total revenue. Moreover, a customized C&CG algorithm according to the special structure of the robust model is developed, and there is no need for primal-dual transformation of subproblems. The key findings can be summarized as follows: (1) the proposed strategy can make the VPP have more arbitrage opportunities in the day-ahead market, resulting in a potential reduction of up to 52.1% in the VPP's total cost compared with the price-taker strategy; (2) the proposed strategy can adapt to more actual scenarios, and has better economy and robustness than the traditional robust model and the two-stage stochastic optimization model; (3) compared with the maximum power of storage, the capacity of storage and the initial SOC have a greater impact on the operating cost of the VPP; (4) the solution algorithm designed by using the special structure of the model can have good computational efficiency, the calculation time can be reduced by about 70% using 6 parallel workers.

The future work will further consider the impact of the uncertainty in the residual energy curves on the VPP's coordinated offering and pricing strategy.

REFERENCES

- [1] S. Babaei, C. Zhao and L. Fan, "A Data-Driven Model of Virtual Power Plants in Day-Ahead Unit Commitment," in *IEEE Transactions on Power Systems*, vol. 34, no. 6, pp. 5125-5135, Nov. 2019, doi: 10.1109/TPWRS.2018.2890714.
- [2] H. Zhao, B. Wang, Z. Pan, H. Sun, Q. Guo and Y. Xue, "Aggregating Additional Flexibility From Quick-Start Devices for Multi-Energy Virtual Power Plants," in *IEEE Transactions on Sustainable Energy*, vol. 12, no. 1, pp. 646-658, Jan. 2021, doi: 10.1109/TSTE.2020.3014959.
- [3] Zamani, Ali Ghahgharaee, Alireza Zakariazadeh, and Shahram Jadid. "Day-ahead resource scheduling of a renewable energy based virtual power plant." in *Applied Energy*, vol. 169, pp. 324-340, 2016.
- [4] H. Saboori, M. Mohammadi and R. Taghe, "Virtual Power Plant (VPP), Definition, Concept, Components and Types," 2011 Asia-Pacific Power and Energy Engineering Conference, Wuhan, China, 2011, pp. 1-4, doi: 10.1109/APPEEC.2011.5749026.
- [5] Elgamal, Ahmed Hany, et al. "Optimization of a multiple-scale renewable energy-based virtual power plant in the UK." in *Applied Energy*, vol. 256, pp. 113973, 2019.
- [6] S. Yu, F.Fang, Y. Liu, et al. "Uncertainties of virtual power plant: Problems and countermeasures." in *Applied energy*, vol. 239, pp. 454-470, 2019.
- [7] E. Mashhour and S. M. Moghaddas-Tafreshi, "Bidding Strategy of Virtual Power Plant for Participating in Energy and Spinning Reserve Markets—Part II: Numerical Analysis," in *IEEE Transactions on Power Systems*, vol. 26, no. 2, pp. 957-964, May 2011, doi: 10.1109/TPWRS.2010.2070883.
- [8] M. Rahimiyan and L. Baringo, "Strategic Bidding for a Virtual Power Plant in the Day-Ahead and Real-Time Markets: A Price-Taker Robust Optimization Approach," in *IEEE Transactions on Power Systems*, vol. 31, no. 4, pp. 2676-2687, July 2016, doi: 10.1109/TPWRS.2015.2483781.
- [9] H. Ding, P. Pinson, Z. Hu and Y. Song, "Optimal Offering and Operating Strategies for Wind-Storage Systems With Linear Decision Rules," in *IEEE Transactions on Power Systems*, vol. 31, no. 6, pp. 4755-4764, Nov. 2016, doi: 10.1109/TPWRS.2016.2521177.

- [10] M. Song and M. Amelin, "Price-Maker Bidding in Day-Ahead Electricity Market for a Retailer With Flexible Demands," in *IEEE Transactions on Power Systems*, vol. 33, no. 2, pp. 1948-1958, March 2018, doi: 10.1109/TPWRS.2017.2741000.
- [11] S. de la Torre, J. M. Arroyo, A. J. Conejo and J. Contreras, "Price maker self-scheduling in a pool-based electricity market: a mixed-integer LP approach," in *IEEE Transactions on Power Systems*, vol. 17, no. 4, pp. 1037-1042, Nov. 2002, doi: 10.1109/TPWRS.2002.804945.
- [12] Z. Yi, Y. Xu, H. Wang and L. Sang, "Coordinated Operation Strategy for a Virtual Power Plant With Multiple DER Aggregators," in *IEEE Transactions on Sustainable Energy*, vol. 12, no. 4, pp. 2445-2458, Oct. 2021, doi: 10.1109/TSTE.2021.3100088.
- [13] G. Liu, Y. Xu and K. Tomovic, "Bidding Strategy for Microgrid in Day-Ahead Market Based on Hybrid Stochastic/Robust Optimization," in *IEEE Transactions on Smart Grid*, vol. 7, no. 1, pp. 227-237, Jan. 2016, doi: 10.1109/TSG.2015.2476669.
- [14] M. Yazdani-Damavandi, N. Neyestani, G. Chicco, M. Shafie-khah and J. P. S. Catalão, "Aggregation of Distributed Energy Resources Under the Concept of Multienergy Players in Local Energy Systems," in *IEEE Transactions on Sustainable Energy*, vol. 8, no. 4, pp. 1679-1693, Oct. 2017, doi: 10.1109/TSTE.2017.2701836.
- [15] Y. Ye, D. Papadaskalopoulos and G. Strbac, "An MPEC approach for analysing the impact of energy storage in imperfect electricity markets," 2016 13th International Conference on the European Energy Market (EEM), Porto, Portugal, 2016, pp. 1-5, doi: 10.1109/EEM.2016.7521287.
- [16] A. Zangeneh, A. Shayegan-Rad, and F. Nazari, "Multi-leader-follower game theory for modelling interaction between virtual power plants and distribution company," in *IET Generation, Transmission & Distribution*, vol. 12, no. 21, pp. 5747-5752, Nov. 2018.
- [17] B. Hu, Y. Gong, C. Y. Chung, B. F. Noble and G. Poelzer, "Price-Maker Bidding and Offering Strategies for Networked Microgrids in Day-Ahead Electricity Markets," in *IEEE Transactions on Smart Grid*, vol. 12, no. 6, pp. 5201-5211, Nov. 2021, doi: 10.1109/TSG.2021.3109111.
- [18] R. Yao, X. Lu, H. Zhou and J. Lai, "A Novel Category-Specific Pricing Strategy for Demand Response in Microgrids," in *IEEE Transactions on Sustainable Energy*, vol. 13, no. 1, pp. 182-195, Jan. 2022, doi: 10.1109/TSTE.2021.3106329.
- [19] D Qiu, Y Wang, J Wang, et al. "Personalized retail pricing design for smart metering consumers in electricity market," in *Applied Energy*, vol. 348, pp. 121545, 2023.
- [20] D Qiu, Z Dong, G Ruan, et al. "Strategic retail pricing and demand bidding of retailers in electricity market: A data-driven chance-constrained programming," in *Advances in Applied Energy*, vol. 7, pp. 100100, 2022.
- [21] Z. Xu, T. Deng, Z. Hu, Y. Song and J. Wang, "Data-Driven Pricing Strategy for Demand-Side Resource Aggregators," in *IEEE Transactions on Smart Grid*, vol. 9, no. 1, pp. 57-66, Jan. 2018, doi: 10.1109/TSG.2016.2544939.
- [22] C. Tang et al., "Look-Ahead Economic Dispatch With Adjustable Confidence Interval Based on a Truncated Versatile Distribution Model for Wind Power," in *IEEE Transactions on Power Systems*, vol. 33, no. 2, pp. 1755-1767, March 2018, doi: 10.1109/TPWRS.2017.2715852.
- [23] C. Tang, J. Xu, Y. Tan, Y. Sun and B. Zhang, "Lagrangian Relaxation With Incremental Proximal Method for Economic Dispatch With Large Numbers of Wind Power Scenarios," in *IEEE Transactions on Power Systems*, vol. 34, no. 4, pp. 2685-2695, July 2019, doi: 10.1109/TPWRS.2019.2891227.
- [24] Y. Chen, Q. Guo, H. Sun, Z. Li, W. Wu and Z. Li, "A Distributionally Robust Optimization Model for Unit Commitment Based on Kullback-Leibler Divergence," in *IEEE Transactions on Power Systems*, vol. 33, no. 5, pp. 5147-5160, Sept. 2018, doi: 10.1109/TPWRS.2018.2797069.
- [25] Mohajerin Esfahani, Peyman, and Daniel Kuhn. "Data-driven distributionally robust optimization using the Wasserstein metric: performance guarantees and tractable reformulations." *Mathematical Programming* 171.1-2 (2018): 115-166.
- [26] D. Ke and C. Y. Chung, "Design of Probabilistically-Robust Wide-Area Power System Stabilizers to Suppress Inter-Area Oscillations of Wind Integrated Power Systems," in *IEEE Transactions on Power Systems*, vol. 31, no. 6, pp. 4297-4309, Nov. 2016, doi: 10.1109/TPWRS.2016.2514520.
- [27] C. Zhao and Y. Guan, "Data-Driven Stochastic Unit Commitment for Integrating Wind Generation," in *IEEE Transactions on Power Systems*, vol. 31, no. 4, pp. 2587-2596, July 2016.
- [28] Z. Tan, H. Zhong, Xia Q et al, "Estimating the robust PQ capability of a technical virtual power plant under uncertainties," in *IEEE Transactions on Power Systems*, vol. 35, no. 6, pp. 4285-4296, Nov. 2020.
- [29] H. Ding, P. Pinson, Z. Hu, J. Wang and Y. Song, "Optimal Offering and Operating Strategy for a Large Wind-Storage System as a Price Maker," in *IEEE Transactions on Power Systems*, vol. 32, no. 6, pp. 4904-4913, Nov. 2017, doi: 10.1109/TPWRS.2017.2681720.
- [30] J. Wang, J. Xu J, D. Ke, et al. "A tri-level framework for distribution-level market clearing considering strategic participation of electrical vehicles and interactions with wholesale market," in *Applied Energy*, vol. 329, pp. 120230, 2023.
- [31] S. Shafiee, H. Zareipour and A. M. Knight, "Developing Bidding and Offering Curves of a Price-Maker Energy Storage Facility Based on Robust Optimization," in *IEEE Transactions on Smart Grid*, vol. 10, no. 1, pp. 650-660, Jan. 2019, doi: 10.1109/TSG.2017.2749437.
- [32] W. Wei, F. Liu and S. Mei, "Energy Pricing and Dispatch for Smart Grid Retailers Under Demand Response and Market Price Uncertainty," in *IEEE Transactions on Smart Grid*, vol. 6, no. 3, pp. 1364-1374, May 2015, doi: 10.1109/TSG.2014.2376522.

- [33] B. Zeng, L. Zhao. "Solving two-stage robust optimization problems using a column-and-constraint generation method,". *Operations Research Letters*, vol. 41, no. 5, pp. 457-461, 2013.
- [34] L. Zhao, B. Zeng. "An exact algorithm for two-stage robust optimization with mixed integer recourse problems." submitted, available on [Optimization-Online. Org](http://Optimization-Online.Org), 2012.
- [35] B. Zhao, J Ren, J Chen, et al. "Tri-level robust planning-operation co-optimization of distributed energy storage in distribution networks with high PV penetration,".in *Applied Energy*, vol. 279, pp. 115768, 2020.